A Space–Time Coding Modem for High-Data-Rate Wireless Communications

Ayman F. Naguib, *Member, IEEE,* Vahid Tarokh, *Member, IEEE,*
Nambirajan Seshadri, *Senior Member, IEEE,* and A. Robert Calderbank, *Fellow, IEEE*

***Abstract*— This paper presents the theory and practice of a new advanced modem technology suitable for high-data-rate wireless communications and presents its performance over a frequency-flat Rayleigh fading channel. The new technology is based on *space–time coded modulation* (STCM) [1]–[5] with multiple transmit and/or multiple receive antennas and *orthogonal pilot sequence insertion* (O-PSI). In this approach, data is encoded by a space–time (ST) channel encoder and the output of the encoder is split into N streams to be simultaneously transmitted using N transmit antennas. The transmitter inserts periodic orthogonal pilot sequences in each of the simultaneously transmitted bursts. The receiver uses those pilot sequences to estimate the fading channel. When combined with an appropriately designed interpolation filter, accurate channel state information (CSI) can be estimated for the decoding process. Simulation results of the proposed modem, as applied to the IS-136 cellular standard, are presented. We present the *frame error rate* (FER) performance results as a function of the signal-to-noise ratio (SNR) and the maximum Doppler frequency, in the presence of timing and frequency offset errors. Simulation results show that for 10% FER, a 32-state eight-phase-shift keyed (8-PSK) ST code with two transmit and two receive antennas can support data rates up to 55.8 kb/s on a 30-kHz channel, at an SNR of 11.7 dB and a maximum Doppler frequency of 180 Hz. Simulation results for other codes and other channel conditions are also provided. We also compare the performance of the proposed STCM scheme with delay-diversity schemes and conclude that STCM can provide significant SNR improvement over simple delay diversity.**

***Index Terms*— Coded modulation, space–time (ST) coding, space–time processing, wireless communications.**

I. Introduction

THE realization of wireless communications, providing high data rate and high quality information exchange between two portable terminals that may be located anywhere in the world, and the vision of a new telephone service based on a single phone that acts as a traditional cellular phone when used outdoors and as a conventional high-quality phone when used indoors [6] has been the new communication challenge in recent years and will continue to be for years to come. The great popularity of cordless phones, cellular phones, radio paging, portable computing, and other personal communication services (PCS's) demonstrates the rising demand for these services. Rapid growth in mobile computing and other wireless data services is inspiring many proposals for high-speed data services in the range of 64–144 kb/s for a microcellular-wide area and high-mobility applications and up to 2 Mb/s for indoor applications [7]. Research challenges in this area include the development of efficient coding and modulation and signal processing techniques to improve the quality and spectral efficiency of wireless communications and better techniques for sharing the limited spectrum among different high-capacity users.

The physical limitations of the wireless channel presents a fundamental technical challenge for reliable communications. The channel is susceptible to time-varying impairments such as noise, interference, and multipath. Limitations on the power and size of the communications and computing devices in a mobile handset are a second major design consideration. Most personal communications and wireless services portables are meant to be carried in a briefcase and/or pocket and must, therefore, be small and lightweight, which translates to a low power requirement since small batteries must be used. Many of the signal processing techniques which may be used for reliable communications and efficient spectral utilization, however, demand significant processing power, precluding the use of low-power devices. Continuing advances in very large scale integration (VLSI) and integrated circuit technology for low power applications will provide a partial solution to this problem. Hence, placing a higher signal processing burden on fixed locations (base stations), with relatively larger power resources than the portables, makes good engineering sense.

Perhaps the single most important factor in providing reliable communications over wireless channels is diversity. Diversity techniques which may be used include time, frequency, and space diversity.

- *Time diversity:* Channel coding in combination with limited interleaving is used to provide time diversity. However, while channel coding is extremely effective in fast-fading environments (high mobility), it offers very little protection under slow fading (low mobility) unless significant interleaving delays can be tolerated.
- *Frequency diversity:* The fact that signals transmitted over different frequencies induce different multipath structures and independent fading is exploited to provide frequency diversity (sometimes referred to as path diversity). In time division multiple access (TDMA) systems, frequency diversity is obtained by the use of equalizers [8] when the multipath delay spread is a significant fraction of a symbol period. The global system for mobile communications (GSM) uses frequency hopping to provide frequency

Manuscript received October 30, 1997; revised March 30, 1998. This paper was presented in part at IEEE GLOBECOM'97, Phoenix, AZ.

The authors are with AT&T Labs-Research, Florham Park, NJ 07932 USA.

Publisher Item Identifier S 0733-8716(98)07895-0.

diversity. In direct sequence code division multiple access (DS-CDMA) systems, RAKE receivers [9], [10] are used to obtain path diversity. When the multipath delay spread is small, as compared to the symbol period, however, frequency or path diversity does not exist.

- *Space diversity:* The receiver/transmitter uses multiple antennas that are separated for reception/transmission and/or differently polarized antennas to create independent fading channels. Currently, multiple antennas at base stations are used for receive diversity at the base. It is difficult, however, to have more than one or two antennas at the portable unit due to the size limitations and cost of multiple chains of RF down conversion.

In this paper we present the theory and practice of a new advanced modem technology suitable for high-data-rate wireless communications based on *space–time coded modulation* (STCM) with multiple transmit antennas [1]–[5] and *orthogonal pilot sequences insertion* (O-PSI). At the transmitter, each block of data is first optionally encoded using a high-rate Reed Solomon (RS) block encoder followed by a *space–time* (ST) channel encoder. The spatial and temporal properties of STCM guarantee that diversity is achieved at the transmitter, while maintaining optional receive diversity, without any sacrifice in transmission rate. The output of the ST encoder is split into N streams that are simultaneously transmitted using N transmit antennas. Each stream of encoded symbols is then independently interleaved, using a block symbol-by-symbol interleaver. The transmitter inserts periodic orthogonal pilot sequences in each one of the simultaneously transmitted blocks. Each block is then pulse-shaped and transmitted from a different antenna. Since the signal at each receive antenna is a linear superposition of the N transmitted signals, the receiver uses the orthogonal pilot sequences to estimate the different fading channels. The receiver then uses an appropriately designed interpolation filter to interpolate those estimates and obtain accurate channel state information (CSI). The interpolated channel estimates, along with the received samples, are then deinterleaved using a block symbol-by-symbol deinterleaver and passed to a vector maximum likelihood sequence decoder, followed by an RS decoder.

The information theoretic aspects of transmit diversity were addressed in [13]–[16]. Previous work on transmit diversity can be classified into three broad categories: schemes using feedback; schemes with feedforward or training information but no feedback; and blind schemes. The first category uses feedback, either explicitly or implicitly, from the receiver to the transmitter to train the transmitter. For instance, in time division duplex (TDD) systems [11], the same antenna weights are used for reception and transmission so that feedback is implicit in the exploitation of channel symmetry. These weights are chosen during reception to maximize the received signal-to-noise ratio (SNR) and, during transmission, to weight the amplitudes of the transmitted signals. Therefore, this will also maximize the SNR at the portable receiver. Explicit feedback includes switched diversity systems with feedback [12]. In practice, however, vehicle movement and interference dynamics cause a mismatch between the channel perceived by the transmitter and that perceived by the receiver.

Transmit diversity schemes mentioned in the second category use linear processing at the transmitter to spread the information across antennas. At the receiver, information is recovered by an optimal receiver. Feedforward information is required to estimate the channel from the transmitter to the receiver. These estimates are used to compensate for the channel response at the receiver. The first scheme of this type was proposed by Wittneben [17] and it includes the delay-diversity scheme of [18] as a special case. The linear processing techniques were also studied in [19] and [20]. It was shown in [21] and [22] that delay-diversity schemes are indeed optimal in providing diversity, in the sense that the diversity gain experienced at the receiver (which is assumed to be optimal) is equal to the diversity gain obtained with receive diversity. The linear filtering used at the transmitter can be viewed as a channel code that takes binary or integer input and creates real valued output. This paper shows that there is a significant gain to be realized by viewing this problem from a coding perspective, rather than from a purely signal processing point of view.

The third category does not require feedback or feedforward information. Instead, it uses multiple transmit antennas combined with channel coding to provide diversity. An example of this approach is the use of channel coding along with phase sweeping [23] or frequency offset [24] with multiple transmit antennas to simulate fast fading. An appropriately designed channel code/interleaver pair is used to provide the diversity benefit. Another approach in this category is to encode information by a channel code and transmit the code symbols, using different antennas, in an orthogonal manner. This can be done by either time multiplexing [23], or by using orthogonal spreading sequences for different antennas [24]. The disadvantage of these schemes, as compared to the previous two categories, is the loss in bandwidth efficiency due to the use of the channel code. Using appropriate coding it is possible to relax the orthogonality requirement needed in these schemes and to obtain the diversity, as well as a coding gain, without sacrificing bandwidth. This will be possible if one views the whole system as a multiple input/multiple output system and uses channel codes that are designed with that view in mind.

Pilot symbol insertion (PSI) has been used to obtain channel estimates for coherent detection and for decoding channel codes over fast flat-fading channels [26]–[32]. The advantage of the PSI technique is that it neither requires complex signal processing nor does it increase the peak factor of the modulated carrier. In [27] through [29] applications and implementations of PS-aided coherent modems are presented. In [26] and [31], the performance of PS-aided coherent modems is studied by theoretical analysis.

The organization of this paper is as follows. In Section II we briefly review the theory of STCM. The reader is referred to [1]–[5] for a detailed treatment of the theory. We present two specific ST codes based on eight-phase-shift keyed (8-PSK) and 16-QAM signaling constellations. We also present an ST code representation for the delay-diversity scheme based on the 8-PSK constellation. These ST codes, as well as the delay-diversity code, will be used in the simulations.

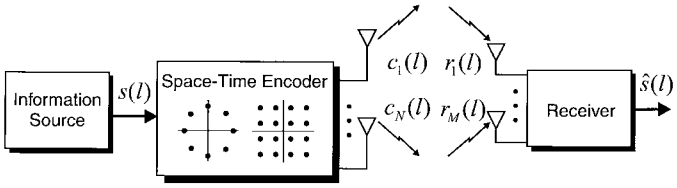

Fig. 1. ST coding.

In Section III, an STCM-based modem architecture and its different signal processing blocks is described. Simulation results for the proposed modem based on 32-state 8-PSK and 16-state 16-quadrature amplitude modulation ST (QAM ST) codes are presented in Section IV. The frame error rate (FER) performance as a function of SNR and maximum Doppler frequency, as well as the effects of antenna correlation and interpolation filter on the FER performance, are examined. In addition, the performance of the 32-state 8-PSK ST code is compared to the performance of the delay-diversity scheme with an 8-PSK constellation. Finally, Section V includes our conclusions and remarks.

II. Space-Time (ST) Coding

In this section we will describe a basic model for a communication system that employs ST coding with N transmit antennas and M receive antennas. As shown in Fig. 1, the information symbol $s(l)$ at time l is encoded by the ST encoder as N code symbols $c_1(l), c_2(l), \cdots, c_N(l)$. Each code symbol is transmitted *simultaneously* from a different antenna. The encoder chooses the N code symbols to transmit, so that both the coding gain and diversity gain are maximized.

Signals arriving at different receive antennas undergo independent fading. The signal at each receive antenna is a noisy superposition of the faded versions of the N transmitted signals. A flat-fading channel is assumed. Let E_s be the average energy of the signal constellation. The constellation points are scaled by a factor of $\sqrt{E_s}$ such that the average energy of the constellation points is 1. Let $r_j(l), j = 1 \cdots M$ be the received signal at antenna j after matched filtering. Assuming ideal timing and frequency information, we have

$$r_j(l) = \sqrt{E_s} \cdot \sum_{i=1}^{N} \alpha_{ij}(l) c_i(l) + \eta_j(l), \quad j = 1, \cdots, M \quad (1)$$

where $\eta_j(l)$ are independent samples of a zero-mean complex white Gaussian process with two-sided power spectral density $N_0/2$ per dimension. It is also assumed that $\eta_j(l)$ and $\eta_k(l)$ are independent for $j \neq k, 1 \leq j,k \leq M$. The gain $\alpha_{ij}(l)$ models the complex fading channel gain from transmit antenna i to receive antenna j. The channel gain α_{ij} is modeled as a low-pass filtered complex Gaussian random process with zero-mean, variance one, and autocorrelation function $R_\alpha(\tau) = J_0(2\pi f_d \tau)$, where $J_0(\cdot)$ is the zeroth-order bessel function of the first kind and f_d is the maximum Doppler frequency [33]. It is also assumed that $\alpha_{ij}(l)$ and $\alpha_{qk}(l)$ are independent for $i \neq q$ or $j \neq k, 1 \leq i,q \leq N, 1 \leq j,k \leq M$. This condition is satisfied if the transmit antennas are well separated (by more than $\lambda/2$) or by using antennas with different polarization.

Let $\boldsymbol{c_l} = [c_1(l), c_2(l), \cdots, c_N(l)]^T$ be the $N \times 1$ code vector transmitted from the N antennas at time l, $\boldsymbol{\alpha}_j(l) = [\alpha_{1j}(l), \alpha_{2j}(l), \cdots, \alpha_{Nj}(l)]^T$ be the corresponding $N \times 1$ channel vector from the N transmit antennas to the jth receive antenna, and $\boldsymbol{r}(l) = [r_1(l), r_2(l), \cdots, r_M(l)]^T$ be the $M \times 1$ received signal vector. Also, let $\boldsymbol{\eta}(l) = [\eta_1(l), \eta_2(l), \cdots, \eta_M(l)]^T$ be the $M \times 1$ noise vector at the receive antennas. Let us define the $M \times N$ channel matrix $\boldsymbol{\mathcal{H}_l}$ from the N transmit to the M receive antennas as $\boldsymbol{\mathcal{H}}(l) = [\boldsymbol{\alpha}_1(l), \boldsymbol{\alpha}_2(l), \cdots, \boldsymbol{\alpha}_M(l)]^T$. Equation (1) can be rewritten in a matrix form as

$$\boldsymbol{r}(l) = \sqrt{E_s} \cdot \boldsymbol{\mathcal{H}}(l) \cdot \boldsymbol{c_l} + \boldsymbol{\eta}(l). \quad (2)$$

We can easily see that the SNR *per receive antenna* is given by

$$\text{SNR} = \frac{N \cdot E_s}{N_o}. \quad (3)$$

A. Performance Criterion

Suppose that the *code vector* sequence

$$\boldsymbol{\mathcal{C}} = \boldsymbol{c}_1, \boldsymbol{c}_2, \cdots, \boldsymbol{c}_L$$

was transmitted. We consider the probability that the decoder decides erroneously in favor of the legitimate code vector sequence

$$\tilde{\boldsymbol{\mathcal{C}}} = \tilde{\boldsymbol{c}}_1, \tilde{\boldsymbol{c}}_2, \cdots, \tilde{\boldsymbol{c}}_L.$$

Assuming that for each frame or block of data of length L the ideal CSI $\boldsymbol{\mathcal{H}}(l), l = 1, \cdots, L$ are available at the receiver, the probability of transmitting $\boldsymbol{\mathcal{C}}$ and deciding in favor of $\tilde{\boldsymbol{\mathcal{C}}}$ is well upper bounded by [34]

$$P(\boldsymbol{\mathcal{C}} \rightarrow \tilde{\boldsymbol{\mathcal{C}}} | \boldsymbol{\mathcal{H}}(l), l = 1, \cdots, L) = Q\left(\sqrt{\frac{\mathcal{D}^2(\boldsymbol{\mathcal{C}}, \tilde{\boldsymbol{\mathcal{C}}}) E_s}{2N_o}}\right) \quad (4)$$

$$\leq \exp\left(-\mathcal{D}^2(\boldsymbol{\mathcal{C}}, \tilde{\boldsymbol{\mathcal{C}}}) \cdot E_s / 4N_o\right) \quad (5)$$

where $Q(x) = (1/\sqrt{2\pi}) \int_x^\infty \exp(-x^2/2)\, dx$ and

$$\mathcal{D}^2(\boldsymbol{\mathcal{C}}, \tilde{\boldsymbol{\mathcal{C}}}) = \sum_{l=1}^{L} ||\boldsymbol{\mathcal{H}}(l)(\boldsymbol{c_l} - \tilde{\boldsymbol{c}}_l)||^2.$$

It is clear that in order to minimize the pairwise error probability we need to maximize $\mathcal{D}^2(\boldsymbol{\mathcal{C}}, \tilde{\boldsymbol{\mathcal{C}}})$ (with the proper design of the ST code). It is clear, however, that $\mathcal{D}^2(\boldsymbol{\mathcal{C}}, \tilde{\boldsymbol{\mathcal{C}}})$ is a function of the maximum Doppler frequency. Therefore, we will derive the performance criterion for designing the ST code, assuming that the fading is static over the block. In this case $\boldsymbol{\mathcal{H}}(l) = \boldsymbol{\mathcal{H}} = [\boldsymbol{\alpha}_1, \boldsymbol{\alpha}_2, \cdots, \boldsymbol{\alpha}_M]^T, l = 1, \cdots, L$ and we can easily verify that

$$\mathcal{D}^2(\boldsymbol{\mathcal{C}}, \tilde{\boldsymbol{\mathcal{C}}}) = \sum_{j=1}^{M} \boldsymbol{\alpha}_j^* \boldsymbol{\mathcal{A}}(\boldsymbol{\mathcal{C}}, \tilde{\boldsymbol{\mathcal{C}}}) \boldsymbol{\alpha}_j \quad (6)$$

where

$$\boldsymbol{\mathcal{A}}(\boldsymbol{\mathcal{C}}, \tilde{\boldsymbol{\mathcal{C}}}) = \sum_{l=1}^{L} (\boldsymbol{c_l} - \tilde{\boldsymbol{c}}_l)(\boldsymbol{c_l} - \tilde{\boldsymbol{c}}_l)^*. \quad (7)$$

We can also verify that the $N \times N$ matrix $\boldsymbol{A}(\boldsymbol{C},\tilde{\boldsymbol{C}})$ is Hermitian and is equal to $\boldsymbol{B}(\boldsymbol{C},\tilde{\boldsymbol{C}})\boldsymbol{B}^*(\boldsymbol{C},\tilde{\boldsymbol{C}})$ where $\boldsymbol{B}(\boldsymbol{C},\tilde{\boldsymbol{C}})$ is $N \times L$ and represents the error sequence $\boldsymbol{C}-\tilde{\boldsymbol{C}}$. The matrix $\boldsymbol{B}$ is a square root of $\boldsymbol{A}$. Since $\boldsymbol{A}$ is Hermitian we can write $\boldsymbol{A}$ as $\boldsymbol{U}\boldsymbol{\Lambda}\boldsymbol{U}^*$ [35] where $\boldsymbol{U}$ is unitary[1] and $\boldsymbol{\Lambda}$ is a diagonal matrix where the diagonal elements $\lambda_n, n = 1, \cdots, N$ are nonnegative and are the eigenvalues of $\boldsymbol{A}$. Therefore, we can write $\mathcal{D}^2(\boldsymbol{C},\tilde{\boldsymbol{C}})$ as

$$\mathcal{D}^2(\boldsymbol{C},\tilde{\boldsymbol{C}}) = \sum_{j=1}^{M} \boldsymbol{\beta}_j^* \boldsymbol{\Lambda} \boldsymbol{\beta}_j \tag{8}$$

where $\boldsymbol{\beta}_j = \boldsymbol{U}^* \boldsymbol{\alpha}_j$. Since $\boldsymbol{U}$ is unitary and $\boldsymbol{\alpha}_j$ is a complex Gaussian random vector with zero mean and covariance $\boldsymbol{I}$, then $\boldsymbol{\beta}_j$ will be also a complex Gaussian random vector with zero mean and covariance $\boldsymbol{I}$. Hence, we will have

$$\mathcal{D}^2(\boldsymbol{C},\tilde{\boldsymbol{C}}) = \sum_{j=1}^{M} \sum_{i=1}^{N} \lambda_i |\beta_{ij}|^2. \tag{9}$$

The random variable $\nu_{ij} = |\beta_{ij}|^2$ has a χ^2 distribution with two degrees of freedom, that is

$$\nu_{ij} \sim f_\nu(\nu) = e^{-\nu} \quad \text{for} \quad \nu > 0 \quad \text{and 0 otherwise.} \tag{10}$$

Thus, to compute an upper bound on the average pairwise error probability we simply average the right-hand side of (5) to arrive at

$$P(\boldsymbol{C} \to \tilde{\boldsymbol{C}}) \leq \left(\prod_{i=1}^{N} \frac{1}{1 + \lambda_i \cdot (E_s/4N_o)} \right)^M. \tag{11}$$

Let r denote the rank of the matrix $\boldsymbol{A}$ (which is also equal to the rank of $\boldsymbol{B}$). Then $\boldsymbol{A}$ has exactly $N - r$ zero eigenvalues. Without loss of generality, let us assume that $\lambda_1, \lambda_2, \cdots, \lambda_r$ are the nonzero eigenvalues, then it follows from (11) that

$$P(\boldsymbol{C} \to \tilde{\boldsymbol{C}}) \leq \left(\prod_{i=1}^{r} \lambda_i \right)^{-M} \cdot (E_s/4N_o)^{-rM}. \tag{12}$$

We can easily see that the probability of error bound in (12) is similar to the probability of error bound for trellis coded modulation for fading channels and, thus, a diversity gain of rM and a coding gain of $g_r = (\lambda_1 \lambda_2 \cdots \lambda_r)^{1/r}$ are achieved [36]. From the above analysis, we arrive at the following design criteria.

- *The Rank Criterion:* In order to achieve the maximum diversity NM, the rank of the matrix $\boldsymbol{B}(\boldsymbol{C},\tilde{\boldsymbol{C}})$ has to be full rank for any two code vector sequences $\boldsymbol{C}$ and $\tilde{\boldsymbol{C}}$. If $\boldsymbol{B}(\boldsymbol{C},\tilde{\boldsymbol{C}})$ has a minimum rank r over the set of two tuples of distinct code vector sequences, then a diversity of rM is achieved.
- *The Determinant Criterion:* Suppose that a diversity benefit rM is our target. The minimum of $g_r = (\lambda_1 \lambda_2 \cdots \lambda_r)^{1/r}$ taken over all pairs of distinct code vector sequences $\boldsymbol{C}$ and $\tilde{\boldsymbol{C}}$ is the coding gain. The design target is to maximize g_r.

[1] An $n \times n$ matrix $\boldsymbol{U}$ is unitary if and only if $\boldsymbol{U}\boldsymbol{U}^* = \boldsymbol{I}$.

B. Maximum Likelihood Vector Decoder

As before, we assume that the ideal CSI $\boldsymbol{\mathcal{H}}(l), l = 1, \cdots, L$ are available at the receiver. We can derive the maximum likelihood decoding rule for the ST code as follows. Suppose that a code vector sequence

$$\boldsymbol{C} = \boldsymbol{c}_1, \boldsymbol{c}_2, \cdots, \boldsymbol{c}_L$$

has been transmitted, and

$$\boldsymbol{\mathcal{R}} = \boldsymbol{r}_1, \boldsymbol{r}_2, \cdots, \boldsymbol{r}_L$$

has been received, where $\boldsymbol{r_l}$ is given by (2). At the receiver, optimum decoding amounts to choosing a vector code sequence

$$\tilde{\boldsymbol{C}} = \tilde{\boldsymbol{c}}_1, \tilde{\boldsymbol{c}}_2, \cdots, \tilde{\boldsymbol{c}}_L$$

for which the *a posteriori* probability

$$\Pr(\tilde{\boldsymbol{C}} | \boldsymbol{\mathcal{R}}, \boldsymbol{\mathcal{H}}(l), l = 1, \cdots, L)$$

is maximized. Assuming that all the code words are equiprobable, and since the noise vector is assumed to be a multivariate allitive white Gaussian noise (AWGN), it can be easily shown that the optimum decoder is [34]

$$\tilde{\boldsymbol{C}} = \arg \min_{\tilde{\boldsymbol{C}} = \tilde{\boldsymbol{c}}_1, \cdots, \tilde{\boldsymbol{c}}_L} \sum_{l=1}^{L} ||\boldsymbol{r}(l) - \sqrt{E_s} \cdot \boldsymbol{\mathcal{H}}(l) \cdot \tilde{\boldsymbol{c}}_l||^2. \tag{13}$$

It is obvious that the optimum decoder in (13) can be implemented using the Viterbi algorithm when the ST code has a trellis representation. In practice, the receiver has to estimate the CSI, and techniques to accurately estimate the multichannel CSI for STCM will be discussed later. CSI estimation errors, however, will limit the performance of STCM. In this case, let $\hat{\boldsymbol{\mathcal{H}}}(l)$ denote the CSI estimate at time l such that

$$\hat{\boldsymbol{\mathcal{H}}}(l) = \boldsymbol{\mathcal{H}}(l) + \boldsymbol{\Delta}_{\mathcal{H}}(l) \tag{14}$$

where the error matrix $\boldsymbol{\Delta}_{\mathcal{H}}(l)$ represents the error in the CSI estimates. The (i,j) element of $\boldsymbol{\Delta}_{\mathcal{H}}(l), e_{ij}(l)$ represents the error in the estimate of the channel gain $\alpha_{ij}(l)$. Since these channels are assumed to be independent, the $e_{ij}(l)$'s are also independent and are modeled as identically distributed Gaussian random variables with zero mean and variance σ_e^2. Moreover, we will also assume that $\{\boldsymbol{\Delta}_{\mathcal{H}}(l)\}_{l=1,\cdots,L}$ are independent. This is true if we assume infinite interleaving depth. For a finite block length, however, these errors will be correlated. In this case we have

$$\boldsymbol{r}_l = \sqrt{E_s} \hat{\boldsymbol{\mathcal{H}}}(l) \boldsymbol{c_l} + \tilde{\boldsymbol{\eta}}(l) \tag{15}$$

where

$$\tilde{\boldsymbol{\eta}}(l) = \boldsymbol{\eta}(l) - \sqrt{E_s} \boldsymbol{\Delta}_{\mathcal{H}}(l) \boldsymbol{c_l}.$$

We can easily verify that $\tilde{\boldsymbol{\eta}}(l)$ is a zero-mean Gaussian random vector with covariance $\Sigma(l) \cdot \boldsymbol{I}$ where

$$\Sigma(l) = N_o + \sqrt{E_s} \sigma_e^2 ||\boldsymbol{c_l}||^2. \tag{16}$$

In this case, and conditioned on $\hat{\boldsymbol{\mathcal{H}}}(l)$, the log likelihood to be minimized for optimum decoding is given by

$$\sum_{l=1}^{L} \{\Sigma^{-1}(l) \cdot ||\boldsymbol{r}(l) - \sqrt{E_s} \cdot \hat{\boldsymbol{\mathcal{H}}}(l) \cdot \boldsymbol{c_l}||^2 + \log \Sigma(l)\}. \tag{17}$$

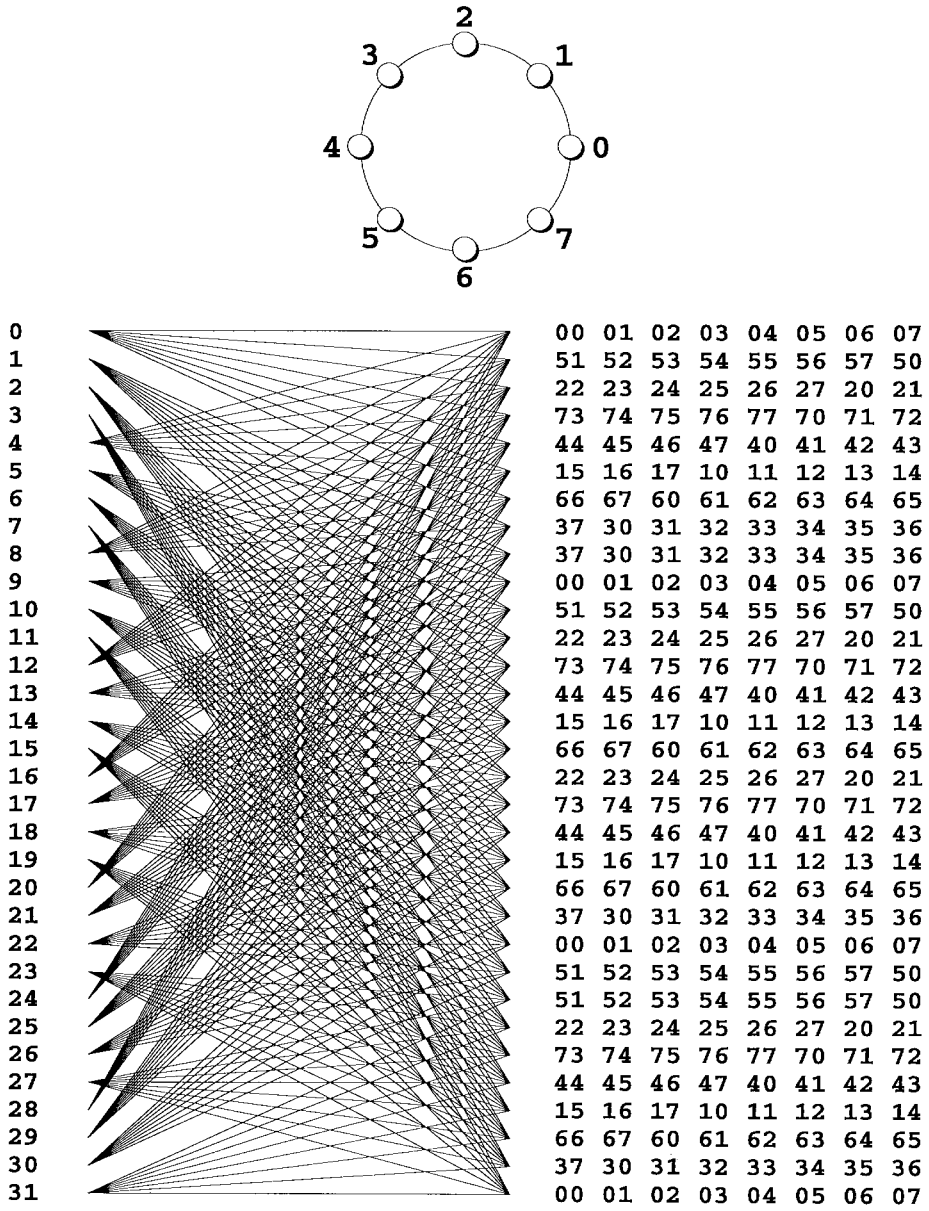

Fig. 2. 8-PSK 32-state ST code with two transmit antennas.

For the case of constant envelope signals such as PSK, $\Sigma(l)$ does not depend on the transmitted code vector $\boldsymbol{c}_l$ and, therefore, the metric in (17) reduces to that in (13), replacing $\boldsymbol{\mathcal{H}}(l)$ with the CSI estimate $\hat{\boldsymbol{\mathcal{H}}}(l)$. This means that the decoding rule in (13) is still optimum for equal energy constellation, e.g., PSK [5], even in the presence of channel estimation errors. For QAM signals, however, this will be true only if we have ideal CSI, or when the channel estimation error is negligible compared to the channel noise, i.e., $E_S\sigma_e^2||\boldsymbol{c}_l||^2 \ll N_o$.

C. Examples of ST Codes

Here we give two examples of ST codes that were designed, using the above criteria, for two transmit antennas. The reader is referred to [1] for further examples of ST codes.

- *Example 1:* Here we provide an 8-PSK 32-state ST code designed for two transmit antennas. Consider the 8-PSK constellation as labeled in Fig. 2. Fig. 2 also shows the trellis description for this code. Each row in the matrix represents the edge labels for transitions from the corresponding state. The edge label s_1s_2 indicates that symbol s_1 is transmitted over the first antenna and that symbol s_2 is transmitted over the second antenna. The input bit stream to the ST encoder is divided into groups of three bits, and each group is mapped into one of eight constellation points. This code has a bandwidth efficiency of 3 bits/channel use.
- *Example 2:* Here we provide a 16-QAM 16-State ST code designed for two transmit antennas. Consider the 16-QAM constellation, as labeled in Fig. 3, using hexadecimal notation. Fig. 3 also shows the trellis description for this code. The input bit stream to the ST encoder is divided into groups of four bits and each group is mapped into one of 16 constellation points. This code has a bandwidth efficiency of 4 bits/channel use.

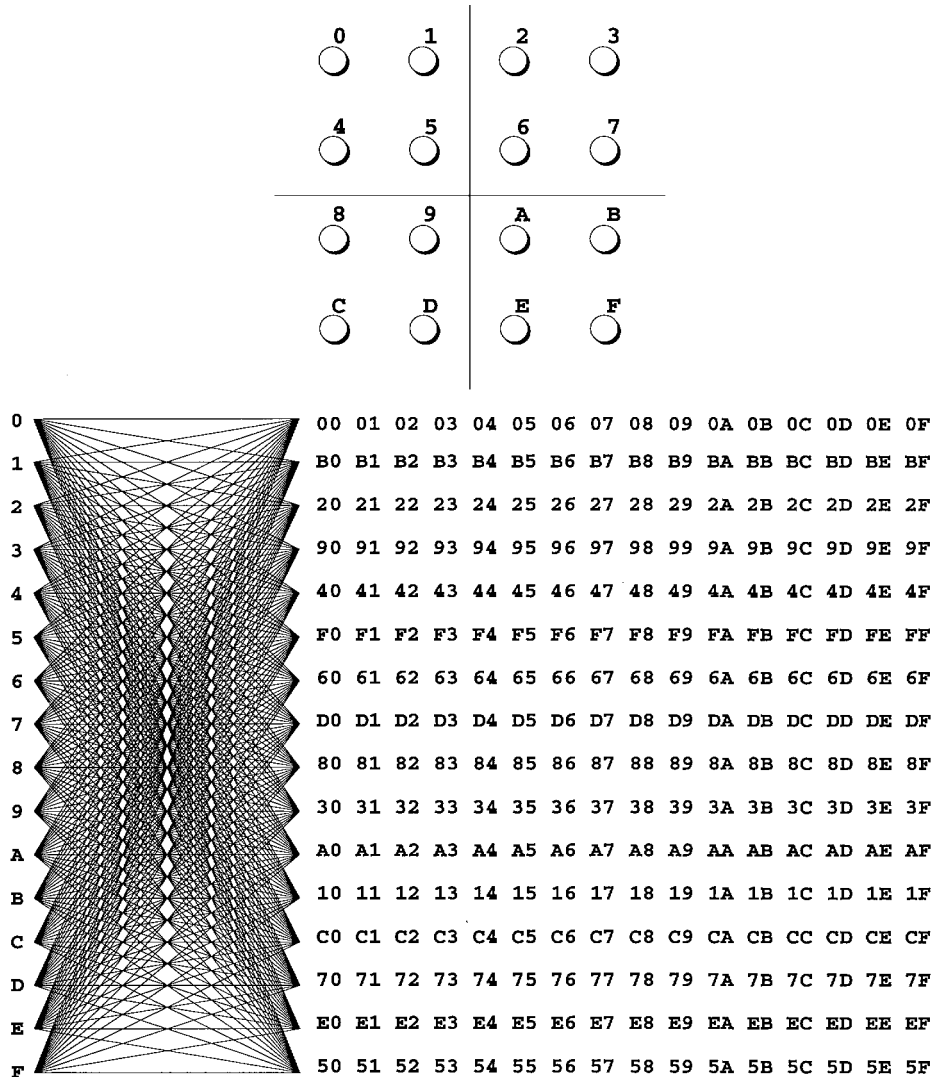

Fig. 3. Sixteen-QAM 16-state ST code with two transmit antennas.

D. Comparison with Delay Diversity

We observe that the delay-diversity scheme of [18] and [19] can be viewed as an ST code and, therefore, the performance analysis presented above applies to it. Consider the delay-diversity scheme of [18] and [19] where the channel encoder is a rate 1/2 block repetition code defined over some signal alphabet. Let $\overline{c}_1(l)\overline{c}_2(l)$ be the output of the channel encoder where $\overline{c}_1(l)$ is to be transmitted from antenna 1 and $\overline{c}_2(l)$ is to be transmitted from antenna two, one symbol later. This can be viewed as an ST code by defining the *code vector* $\boldsymbol{c}(l)$ as

$$\boldsymbol{c}_l = \begin{pmatrix} \overline{c}_1(l) \\ \overline{c}_2(l-1) \end{pmatrix}. \tag{18}$$

Now, let us consider the 8-PSK constellation in Fig. 4. It is easy to show that the ST code realization of this delay-diversity scheme has the trellis representation in Fig. 4. The minimum determinant of this code is $(2-\sqrt{2})^2$.

Next, consider the block code

$$\boldsymbol{C} = \{00, 15, 22, 37, 44, 51, 66, 73\} \tag{19}$$

of length two defined over the 8-PSK alphabet instead of the repetition code. This block code is the best, in the sense of product distance [18], among all the codes of cardinality eight and of length two, defined over the 8-PSK alpha-

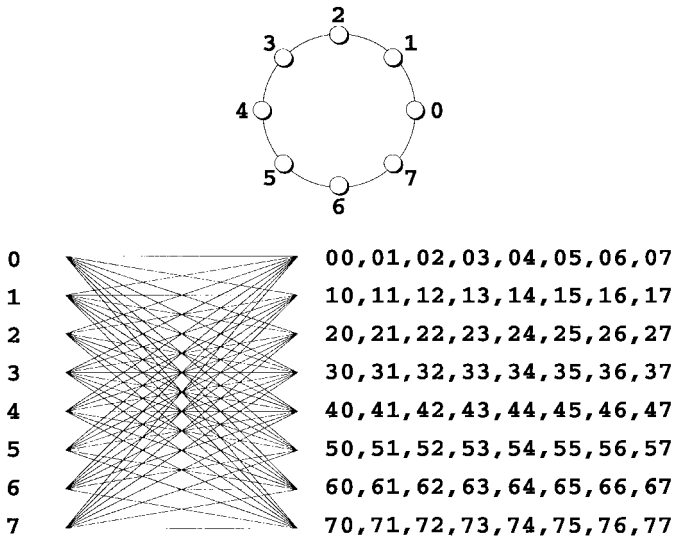

Fig. 4. ST coding realization of a delay-diversity 8-PSK eight-state code with two transmit antennas.

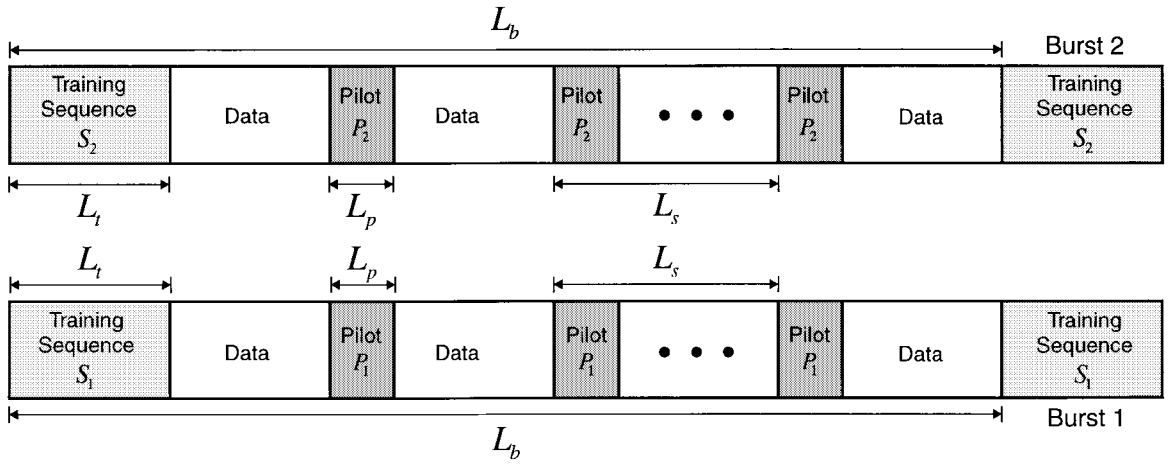

Fig. 5. Downlink slot structure for STCM-based modem.

bet. This means that the minimum of the product distance $|c_1 - \tilde{c}_1||c_2 - \tilde{c}_2|$ between pairs of distinct code words $\boldsymbol{c} = c_1c_2 \in \boldsymbol{\mathcal{C}}$ and $\tilde{\boldsymbol{c}} = \tilde{c}_1\tilde{c}_2 \in \boldsymbol{\mathcal{C}}$ is the maximum among all such codes. The delay-diversity code constructed from this repetition code is identical to the 8-PSK eight-state ST code [1]. The minimum determinant of this code is two. Simulation results in Section IV will show an advantage of up to 9 dB for the proposed ST coded modulation scheme with the 8-PSK 32-state ST code, over the delay-diversity code with 8-PSK (obtained by the use of repetition code).

III. System Architecture

In this section, we will present a general architecture for a narrowband TDMA/STCM-based modem with N transmit antennas suitable for wireless communications. Without loss of generality, we will assume that $N = 2$. For brevity, we will also present the modem architecture for the downlink only. The uplink modem will have a similar architecture, except that the framing and timing structure will be different and must allow for a guard time between different asynchronous (due to difference in propagation delay) bursts from different users. The transmit antennas are assumed to be placed far enough apart so that each transmit signal will experience independent fading. Independent fading may be also obtained by the use of two dually polarized transmit antennas.

A. Timing and Framing Structure

The system architecture that we propose is similar, but not identical, to that of the IS-136 US cellular standard. Let W be the bandwidth of each of the frequency channels, R_s be the raw symbol rate, N_f be the number of TDMA frames per second for each frequency channel, and N_s be the number of time slots per TDMA frame. Fig. 5 shows the basic TDMA time slot structure. A signaling format which interleaves training and synchronization sequences, pilot sequences, and data is used. In each TDMA slot two bursts are transmitted, one from each antenna. Each burst is L_b symbols long and begins with a training sequence of length L_t symbols. The training sequences $\boldsymbol{S}_1$ and $\boldsymbol{S}_2$ will be used for timing and frequency synchronization at the receiver. In addition, every L_s symbols, the transmitter inserts N_p pilot sequences $\boldsymbol{P}_1$ and $\boldsymbol{P}_2$, each, of length L_p symbols. The length of the pilot sequences L_p should be at least equal to the number of transmit antennas N. In addition, we may note that the symbols used for pilots do not necessarily belong to the same symbol alphabet used for sending the information symbols. Without loss of generality, we will assume that the pilot and synchronization symbols are taken from a constant envelope constellation (8-PSK or $\pi/4$-shifted differential PSK (DPSK), for example). The pilot sequences $\boldsymbol{P}_1$ and $\boldsymbol{P}_2$, along with the training sequences $\boldsymbol{S}_1$ and $\boldsymbol{S}_2$, will be used at the receiver to estimate the channel from each of the transmit antennas to the receiver. *In general, with N transmit antennas we will have N different synchronization sequences $\boldsymbol{S}_1, \boldsymbol{S}_2, \cdots, \boldsymbol{S}_N$, and N different pilot sequences $\boldsymbol{P}_1, \boldsymbol{P}_2, \cdots, \boldsymbol{P}_N$.* Since signals at the receiver antennas will be linear superpositions of all transmitted signals, we choose the training sequences $\boldsymbol{S}_1$ and $\boldsymbol{S}_2$ and the pilot sequences $\boldsymbol{P}_1$ and $\boldsymbol{P}_2$ to be orthogonal sequences. Thus, the number of data symbols L_d in each burst is

$$L_d = L_b - L_t - N_p \cdot L_p. \tag{20}$$

B. Transmitter Model

Fig. 6 shows a block diagram for the transmitter where, in addition to the ST encoder, a high-rate RS block encoder is used as an outer code. The reason for using an outer block code is that, as it will be seen later from the simulation, at reasonable values of SNR, when only the ST code is used most of the frame errors are due to very few symbol errors per frame, most of which can be recovered by the use of an outer block code. The overall coding strategy of the modem is called *concatenated ST coding*. Depending on the desired error correction capability of the RS code, its rate, and the signal constellation used, the dimensions of the RS code should be chosen so that we have an integer number of RS code words per one TDMA slot. In this case we will be able to decode each slot immediately, without the need to wait for other bursts, thereby minimizing the decoding delay.

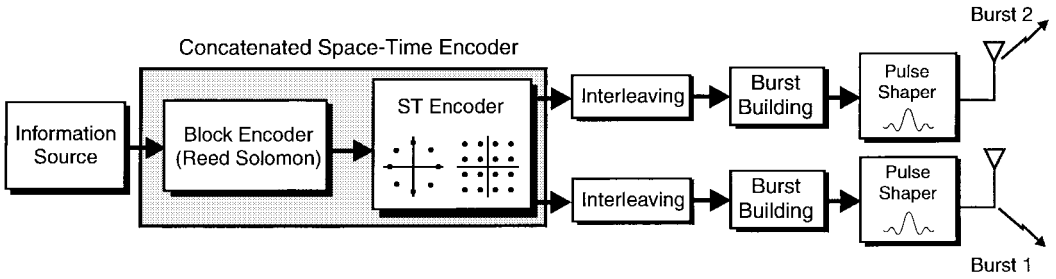

Fig. 6. Base station transmitter with STCM and two transmit antennas.

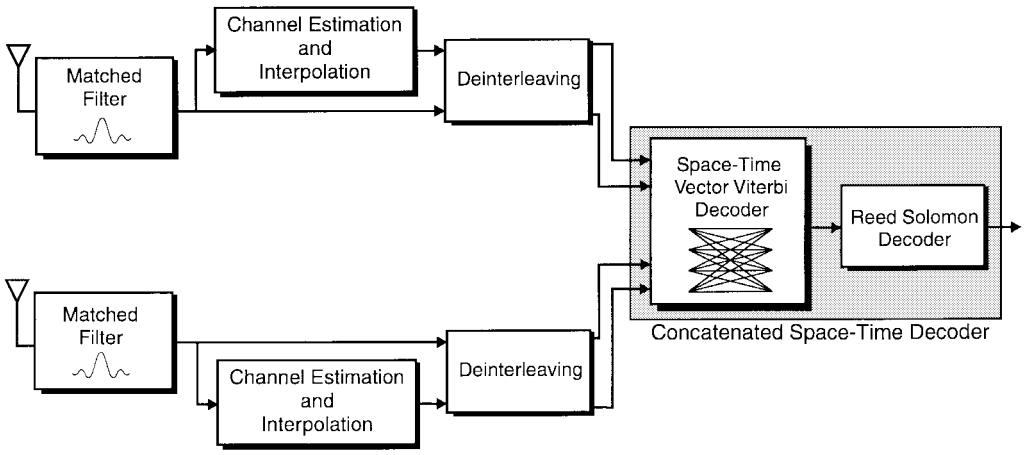

Fig. 7. Mobile receiver with STCM and two receive antennas.

Let B be the number of information bits/modulation symbols. We assume that the RS code used is a (N_c, K_c) code over $GF(2^q)$. The K_c $GF(2^q)$ symbols are first created by partitioning a block of $q \cdot K_c$ information bits into K_c groups of q bits, each. Similarly, the N_c $GF(2^q)$ output symbols are split into $L_d = (q \cdot N_c/B)$ modulation symbols. Thus, the data throughput of the system is

$$\rho_d = \frac{K_c}{N_c} \cdot \left(1 - \frac{L_t + N_p \cdot L_p}{L_b}\right). \tag{21}$$

The output of the RS encoder is then encoded by an ST channel encoder and the output of the ST encoder is split into two streams of encoded modulation symbols. Each stream of encoded symbols is then independently interleaved using a block symbol-by-symbol interleaver. The transmitter inserts the corresponding training and periodic pilot sequences in each of the two bursts. Each burst is then pulse-shaped and transmitted from the corresponding antenna. In this case, we can write the signal transmitted from the ith antenna, $i = 1, 2$, as

$$s_i(t) = \sqrt{E_s} \cdot \sum_l c_i(l) p(t - lT_s) \tag{22}$$

where $T_s = 1/R_s$ is the symbol period and $p(t)$ is the transmit filter pulse shaping function. Without loss of generality, we will assume that $p(t)$ is a square root raised-cosine $(\sqrt{\text{RC}})$ pulse shape given by [34]

$$p(t) = \frac{4\epsilon}{\pi\sqrt{T_s}} \cdot \frac{\cos((1+\epsilon)\pi t/T_s) + \dfrac{\sin((1-\epsilon)\pi t/T_s)}{(4\epsilon t/T_s)}}{(4\epsilon t/T_s)^2 - 1} \tag{23}$$

where ϵ is the bandwidth expansion or roll-off factor. Since $p(t)$ is noncausal, we truncate $p(t)$ to $\pm 3T_s$ around $t = 0$.

C. Receiver Model

Fig. 7 shows the corresponding block diagram of a mobile receiver equipped with two receive antennas. After down conversion to baseband, the received signal at each antenna element is filtered using a receive filter with impulse response $\overline{p}(t)$ that is matched to the transmit pulse shape $p(t)$. In the case of a $\sqrt{\text{RC}}$ transmit filter, $\overline{p}(t) = p(t)$. The output of the matched filters is over sampled at a rate f_{AD} that is Q times faster than the symbol rate R_s, that is, $f_{AD} = Q \cdot R_s$. Received samples corresponding to the training sequences $\boldsymbol{S}_1$ and $\boldsymbol{S}_2$ are used for timing and frequency synchronization. The received samples at the optimum sampling instant are then split into two streams. The first one contains the received samples corresponding to the pilot and training symbols. These are used to estimate the corresponding CSI $\hat{\boldsymbol{\mathcal{H}}}(l)$ at the pilot and training sequence symbols. The receiver then uses an appropriately designed interpolation filter to interpolate those trained CSI estimates and obtain accurate interpolated CSI estimates for

the whole burst. The second stream contains the received samples corresponding to the superimposed information symbols. The interpolated CSI estimates, along with the received samples corresponding to the information symbols, are then deinterleaved using a block symbol-by-symbol deinterleaver and passed to a vector maximum likelihood sequence decoder, followed by an RS decoder.

D. Received Signal Model

We can write the received signal at the jth antenna, $r_j(t)$, as

$$r_j(t) = \sqrt{E_s} \cdot \sum_{i=1}^{N} \tilde{\alpha}_{ij}(t) \sum_n c_i(n) p(t - nT_s) + \eta_j(t) \tag{24}$$

where the overall complex channel variable $\tilde{\alpha}_{ij}(t)$ incorporates both the channel gain and the effect of the residual frequency offset and is given by

$$\tilde{\alpha}_{ij}(t) = \alpha_{ij}(t) e^{j2\pi f_o t} \tag{25}$$

where f_o is the residual frequency offset after automatic frequency control (AFC). We can easily see that $\tilde{\alpha}_{ij}(t)$ is bandlimited to $f_o + f_d$. The autocorrelation function of $\tilde{\alpha}_{ij}(t)$ is given by

$$R_{\tilde{\alpha}}(\tau) = J_o(2\pi f_d \tau) e^{j2\pi f_o \tau}. \tag{26}$$

Define $y_j(t)$ as the matched filter output at the jth antenna, which is given by[2]

$$\begin{aligned} y_j(t) &= \int r_j(\tau) p(t - \tau)\, d\tau \\ &= \sqrt{E_s} \cdot \sum_{i=1}^{N} \tilde{\alpha}_{ij}(t) \sum_n c_i(n) \tilde{p}(t - nT_s) + \overline{\eta}_j(t) \end{aligned} \tag{27}$$

where $\tilde{p}(t) = p(t) * p(t)$ is the raised-cosine pulse shape and the colored noise $\overline{\eta}_j(t)$ is given by

$$\overline{\eta}_j(t) = \int \eta_j(\tau) p(t - \tau)\, d\tau. \tag{28}$$

We note that $\overline{\eta}_j(t)$ has a zero mean and an autocorrelation of

$$R_\eta(t_1 - t_2) = N_o \cdot \tilde{p}(t_1 - t_2). \tag{29}$$

For $|t_1 - t_2| = lT_s$ where l is an integer, we have $R_\eta(lT_s) = N_o$ for $l = 0$ and 0 otherwise. Thus, the noise at the output of the matched filter will be uncorrelated when sampled at the symbol rate.

[2]Here we have ignored the intersymbol interference (ISI) due to the time varying nature of the fading, which is a reasonable assumption to make when the fading bandwidth is much smaller than the pulse shape bandwidth.

As we mentioned earlier, the output of the matched filter will be sampled at a rate f_{AD} that is Q times faster than the symbol rate R_s, that is $f_{AD} = Q \cdot R_s$. Let us assume that the sampling time for A/D conversion is

$$t_{l,k} = lT_s + \frac{k}{Q} T_s + \delta T_s \tag{30a}$$

$$l = 1, 2, \cdots \tag{30b}$$

$$k = 0, 1, 2, \cdots, Q - 1 \tag{30c}$$

where δT_s is the timing error. Therefore, we can write the samples at the jth antenna matched filter output as

$$\begin{aligned} y_j(t_{l,k}) = \sqrt{E_s} \cdot \sum_{i=1}^{N} \tilde{\alpha}_{ij}(t_{l,k}) c_i(l) \tilde{p}(t_{l,k} - lT_s) \\ + v_j(t_{l,k}) + \overline{\eta}_j(t_{l,k}) \end{aligned} \tag{31}$$

where $v_j(t_{l,k})$ represents the intersymbol interference (ISI) due to other transmitted symbols and is given by

$$v_j(t_{l,k}) = \sqrt{E_s} \cdot \sum_{i=1}^{N} \tilde{\alpha}_{ij}(t_{l,k}) \sum_{n \neq l} c_i(n) \cdot \tilde{p}(t_{l,k} - nT_s). \tag{32}$$

In addition, when the fading bandwidth is much smaller than the reciprocal of the symbol period it is reasonable to assume that the fading is constant over one symbol period, that is

$$\tilde{\alpha}_{ij}(t_{l,k}) \approx \tilde{\alpha}_{ij}(t_{l,0}) = \tilde{\alpha}_{ij}(lT_s) = \tilde{\alpha}_{ij}(l).$$

In this case, we can rewrite $y_j(t_{l,k})$ as

$$\begin{aligned} y_j(l,k) &= y_j(t_{l,k}) \\ &= \sqrt{E_s} \cdot \tilde{\alpha}_{ij}(l) \cdot \sum_{i=1}^{N} c_i(l) \tilde{p}(t_{l,k} - lT_s) \\ &\quad + v_j(t_{l,k}) + \overline{\eta}_j(t_{l,k}). \end{aligned} \tag{33}$$

E. Timing and Frequency Synchronization

A frequency offset in the order of 1 ppm, which corresponds to 1.9 kHz at a carrier frequency of 1.9 GHz, will exist in the baseband signal. This frequency offset can be coarsely compensated for using an AFC circuit [37]. After the coarse frequency offset compensation, a residual frequency offset f_o in the order of 0.1 ppm will still exist in the baseband signal and can be compensated for, as we will see later, as part of the channel estimation [38].

For symbol timing synchronization the receiver uses the $Q \times L_t$ samples, corresponding to the training symbols as follows. Consider the jth antenna signal at the output of the matched filter, as given by (33). First, we make the reasonable assumption that the channel is almost constant over the duration of the training sequence and is equal to the value of the channel in the middle of the training period, that is, $\tilde{\alpha}_{ij}(0) \approx \tilde{\alpha}_{ij}(L_t - 1) = \tilde{\alpha}_{ij}(L_t/2)$. Also, let us define the overall

noise term as $z_j(l,k) = z_j(t_{k,l}) = v_j(t_{k,l}) + \overline{\eta}_j(t_{k,l})$. Let us consider the received samples $y_j(0,k), y_j(1,k), \cdots, y_j(L_t - 1, k)$. Let $\tilde{p}(l,k) = \tilde{p}(t_{l,k} - lT_s)$. Then, we may note that $\tilde{p}(0,k) = \tilde{p}(1,k) = \cdots = \tilde{p}(L_t - 1, k) = \tilde{p}(kT_s/Q)$. Define $\boldsymbol{X}_j(k)$ as

$$\begin{aligned}
&\boldsymbol{X}_j(k) \\
&\quad = [y_j(0,k,0) y_j(1,k) \cdots y_j(L_t - 1, k)]^T \\
&\quad = A_s(k) \begin{bmatrix} c_1(0) & c_2(0) & \cdots & c_N(0) \\ c_1(1) & c_2(1) & \cdots & c_N(1) \\ \vdots & \vdots & \vdots & \vdots \\ c_1(L_t-1) & c_2(L_t-1) & \cdots & c_N(L_t-1) \end{bmatrix} \\
&\qquad \cdot \begin{bmatrix} \tilde{\alpha}_{1j}(L_t/2) \\ \tilde{\alpha}_{2j}(L_t/2) \\ \vdots \\ \tilde{\alpha}_{Nj}(L_t/2) \end{bmatrix} + \begin{bmatrix} z_j(0,k) \\ z_j(1,k) \\ \vdots \\ z_j(L_t-1,k) \end{bmatrix} \\
&\quad = A_s(k)[\boldsymbol{S}_1 \quad \boldsymbol{S}_2 \quad \cdots \quad \boldsymbol{S}_N]\tilde{\boldsymbol{\alpha}}_j(L_t/2) + \boldsymbol{z}_j(k) \qquad (34)
\end{aligned}$$

where $A_s(k) = \sqrt{E_s}\tilde{p}(kT_s/Q)$. We assume (erroneously[3]) that the noise term due to ISI $v_j(l,k) = v_j(lT_s + kT_s/Q)$ is modeled as uncorrelated Gaussian noise with zero mean and variance $\sigma_v^2(k)$. Therefore, the overall noise vector $\boldsymbol{z}_k$ is zero mean with covariance $\sigma_z^2(k)\boldsymbol{I}$ where $\sigma_z^2(k) = \sigma_v^2(k) + N_o$. Define $\Psi_{ij}(k) = \boldsymbol{S}_i^* \boldsymbol{X}_j(k)$. Since the training sequences are orthogonal, it is easy to verify that

$$\Psi_{ij}(k) = A_s(k)\tilde{\alpha}_{ij}(L_t/2)||\boldsymbol{S}_i||^2 + \overline{z}_{ij}(k) \qquad (35)$$

where $\overline{z}_{ij}(k) = \boldsymbol{S}_i^* \boldsymbol{z}_j(k)$. The symbol timing synchronization algorithm estimates which k is closest to the optimum sampling instant in each frame. This value of k can be estimated using maximum likelihood estimation. Similar to the development in [40], we can shows that the log likelihood function for the symbol timing synchronization can be approximated by

$$\Lambda_{\mathrm{ML}}(k) = \sum_{j=1}^{M}\sum_{i=1}^{N} \Lambda_{ij}(k) = \sum_{j=1}^{M}\sum_{i=1}^{N} |\Psi_{ij}(k)|^2, \quad k = 0, 1, \cdots, Q-1. \qquad (36)$$

The optimum sampling instant k^* is obtained by searching for the value k that gives the maximum value of $\Lambda_{ML}(k)$. Because in (36) we only use the envelope of $\Psi_{ij}(k)$, this method will be robust against phase distortion due to the Rayleigh fading, especially in deep fades.

F. Channel Estimation

Consider the jth receive antenna output after matched filtering. We can write the received signal samples for the lth symbol within the burst at the optimum sampling instant as

$$y_j(l) = \sqrt{E_s}\tilde{p}(\delta T_s') \sum_{i=1}^{N} \tilde{\alpha}_{ij}(l) c_i(l) + v_j(l) + \overline{\eta}_j(l) \qquad (37)$$

where $\delta T_s'$ is the timing error after timing synchronization, $\overline{\eta}_j(l)$ is the AWGN with zero mean and variance $N_o/2$ per dimension, and $v_j(l)$ is the ISI due to the timing error which is modeled as uncorrelated Gaussian noise with zero mean and variance σ_v^2.

Consider the output samples corresponding to the nth pilot sequence within the burst $y_j((n-1)L_s + 1), y_j((n-1)L_s + 2), \cdots, y_j((n-1)L_s + L_p)$. As before, a reasonable assumption to make is that the channel is almost constant over the duration of the pilot sequence and is equal to the value of the channel in the middle of the pilot sequence, that is, $\tilde{\alpha}_{ij}(n) = \tilde{\alpha}_{ij}((n-1)L_s + 1) \approx \tilde{\alpha}_{ij}((n-1)L_s + L_p) = \tilde{\alpha}_{ij}((n-1)L_s + L_p/2)$. As before, we define the overall noise term as $z_j(n) = \overline{\eta}_j(n) + v_j(n)$. Define $\boldsymbol{Y}_j(n)$ as

$$\begin{aligned}
\boldsymbol{Y}_j(n) &= [y_j((n-1)L_s + 1) y_j((n-1)L_s + 2) \\
&\qquad \cdots y_j((n-1)L_s + L_p)]^T \\
&= A_s \begin{bmatrix} c_1(1) & c_2(1) & \cdots & c_N(1) \\ c_1(2) & c_2(2) & \cdots & c_N(2) \\ \vdots & \vdots & \cdots & \vdots \\ c_1(L_p) & c_2(L_p) & \cdots & c_N(L_p) \end{bmatrix} \\
&\qquad \cdot \begin{bmatrix} \tilde{\alpha}_{1j}(n) \\ \tilde{\alpha}_{2j}(n) \\ \vdots \\ \tilde{\alpha}_{Nj}(n) \end{bmatrix} + \begin{bmatrix} z_j((n-1)Ls + 1) \\ z_j((n-1)Ls + 2) \\ \vdots \\ z_j((n-1)L_s + L_p) \end{bmatrix} \\
&= A_s[\boldsymbol{P}_1 \quad \boldsymbol{P}_2 \quad \cdots \quad \boldsymbol{P}_N]\tilde{\boldsymbol{\alpha}}_j(n) + \boldsymbol{z}_j(n) \qquad (38)
\end{aligned}$$

where $A_s = \sqrt{E_s}\tilde{p}(\delta T_s')$. Using the fact that $\boldsymbol{P}_1, \boldsymbol{P}_2, \cdots, \boldsymbol{P}_N$ are orthogonal, we can immediately see that the minimum mean square error (MMSE) estimate of $\tilde{\alpha}_{ij}(l)$ is given by

$$\hat{\tilde{\alpha}}_{ij}(l) = \frac{\boldsymbol{P}_i^* \boldsymbol{Y}_j(n)}{A_s \cdot ||\boldsymbol{P}_i||^2}, \qquad i = 1, 2, \cdots, N. \qquad (39)$$

It is easy to show that

$$\hat{\tilde{\alpha}}_{ij}(n) = \tilde{\alpha}_{ij}(n) + e_{ij}(n) \qquad (40)$$

where $e_{ij}(n)$ is the estimation error due to the noise and ISI and is given by

$$e_{ij}(n) = \frac{\boldsymbol{P}_i^* \boldsymbol{z}_j(l)}{A_s \cdot ||\boldsymbol{P}_i||^2}, \qquad i = 1, 2, \cdots, N. \qquad (41)$$

Since $\boldsymbol{z}_j(n)$ is assumed to be a zero-mean Gaussian random vector it easy to see that $e_{ij}(n)$ will be also Gaussian with zero mean and variance

$$\sigma_e^2(n) = \frac{\sigma_v^2 + N_o}{A_s^2 \cdot ||\boldsymbol{P}_i||^2}. \qquad (42)$$

Note that, in the case of pilot symbols with constant envelope, $||\boldsymbol{P}_i||^2 = L_p$ and in this case we will have

$$\sigma_e^2(n) = \frac{\sigma_v^2 + N_o}{A_s^2 \cdot L_p}. \qquad (43)$$

At nominal SNR's, and when the timing error is relatively small, the variance of the term due to ISI will be very small as compared to the thermal noise variance, that is, $\sigma_v^2 \ll N_o$. In addition, we will have $A_s^2 \approx E_s$. In this case, the variance of the estimation error will be given by

$$\sigma_e^2 \approx \frac{1}{(E_s/N_o) \cdot L_p}. \qquad (44)$$

[3]This approximation is only valid if the code symbols are Gaussian [39] and if the timing error is constant, but otherwise unknown.

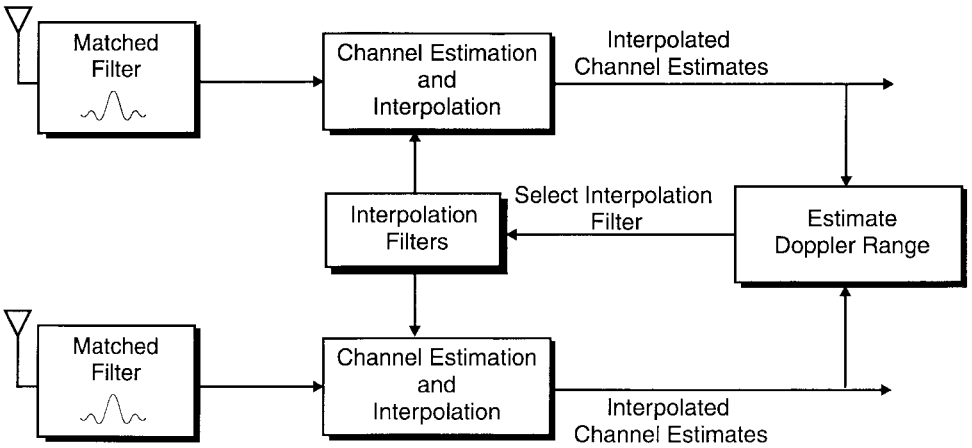

Fig. 8. Quasi-adaptive channel interpolation.

In order to minimize the overall system delay we will assume that the receiver estimates the CSI in any given time slot using the pilot and training sequences in that slot only. Therefore, we will avoid the need to wait for future bursts in order to be able to estimate the channel and perform the decoding of the slot. In addition, other time slots may be carrying bursts that correspond to old IS-136 wireless channels or any other bursts with different slot structure and, thus, no pilot symbols will exist in those slots.

G. Channel Interpolation

Without loss of generality, let us assume that the number of trained channel estimates in each time slot is N_e. For clarity of notation, let $h_{ij}(n)$ denote the trained channel estimate $\{\hat{\tilde{\alpha}}_{ij}(n), n = 1, \cdots, N_e\}$. These trained channel estimates need to be interpolated to obtain a complete CSI for the whole time slot. To satisfy the Nyquist criterion, the normalized sampling rate of the trained channel estimates must satisfy

$$\overline{f}_s' = \frac{f_s'}{2(f_d + f_o)} = \frac{1}{(L_s \cdot T_s) \cdot 2(f_o + f_d)} \geq 1. \tag{45}$$

Moreover, in order to compensate for the fact that, in estimating the channel over any time slot, we are using the pilot and training symbols in that time slot only, $\overline{f}_s'$ should be slightly higher than one. Here, we will briefly consider two different approaches for interpolating the channel estimates.

1) Wiener Interpolation Filter (WIF): In this approach, we use a multichannel generalization of the WIF proposed in [26]. In this case, the receiver estimates the channel gain $\tilde{\alpha}_{ij}(l), 1 \leq i \leq N, 1 \leq j \leq M$ for the lth symbol position in the burst as a linear combination of the trained channel estimates

$$\hat{\tilde{\alpha}}_{ij}(l) = \sum_{n=1}^{N_e} w^*(n,l) h_{ij}(n) = \boldsymbol{w}^*(l) \boldsymbol{h}_{ij} \tag{46}$$

where $\boldsymbol{w}(l) = [w(1,l) \quad w(2,l) \quad \cdots \quad w(N_e,l)]^T$ and $\boldsymbol{h}_{ij} = [h_{ij}(1) \quad h_{ij}(2) \quad \cdots \quad h_{ij}(N_e)]^T$. Note that the interpolator coefficients $\boldsymbol{w}(l)$ are different for every symbol position in the burst. These coefficients are chosen such that the mean squared error (MSE) between the channel gain $\tilde{\alpha}_{ij}(l)$ and its *interpolated* estimate $\hat{\tilde{\alpha}}_{ij}(l)$ is minimized. In this case, it is known that the optimum interpolator coefficients are given by the Wiener solution [41]

$$\boldsymbol{w}(l) = \boldsymbol{R}_h^{-1} \boldsymbol{a}(l) \tag{47}$$

where $\boldsymbol{R}_h$ is an $N_e \times N_e$ matrix and $\boldsymbol{a}(l)$ is an $N_e \times 1$ vector and are given by

$$\boldsymbol{R}_h = E\{\boldsymbol{h}_{ij} \boldsymbol{h}_{ij}^*\} \quad \text{and}$$
$$\boldsymbol{a}(l) = E\{\tilde{\alpha}_{ij}^*(l) \boldsymbol{h}_{ij}\}.$$

From (26) and (40) we can easily see that the (m,n) element of $\boldsymbol{R}_h$ and the nth element of $\boldsymbol{a}(l)$ are given by

$$R_{h,mn} = \sigma_e^2 + J_o(2\pi f_d (m-n) T_s) e^{j2\pi f_o (m-n) T_s} \quad \text{and}$$
$$a_n(l) = J_o(2\pi f_d (l-n) T_s) e^{j2\pi f_o (l-n) T_s}$$

respectively. In this case, we can easily show that the MMSE in the interpolated estimates $\sigma_i^2(l)$ is given by

$$\sigma_{ij}^2(l) = \sigma_\alpha^2 - \boldsymbol{a}^*(l) \boldsymbol{w}(l) \tag{48}$$

where σ_α^2 is the variance of $\alpha_{ij}(l)$ which was assumed to be one.

As in [26], however, the optimum WIF assumes knowledge of the SNR (or more specifically the estimation error variance σ_e^2 which can be related to the SNR, as shown above), the maximum Doppler frequency f_d, and the residual frequency offset f_o and therefore will be different for different values of the SNR, f_d and f_o. This would be very complex for practical implementation. In a practical scenario, the filter will be optimized for the worst case f_d and f_o such that it will have a bandwidth that is wide enough for all possible time variations of the channel. In this case, however, the performance at low f_d and f_o will be the same as that of the worst case (noise in the interpolated estimates will have a larger variance due to the large bandwidth of the interpolation filter). In addition, if $f_d + f_o$ exceeds the filter bandwidth, aliasing in the interpolated CSI will occur and we will have a significant mismatch between the interpolated CSI and the ideal one. This will lead to a significant error floor. Here, we consider a quasi-adaptive approach to remedy this problem. This approach is shown in Fig. 8. In this approach, we divide the range of all

possible f_d into different nonoverlapping ranges. For every range of Doppler frequencies, we design an optimum WIF for the maximum Doppler frequency in that range and use it for the whole range. By observing the correlations of the interpolated channel estimates from the previous time slots, or by observing its frame error rate (FER), the receiver selects which filter to use.

2) Low-Pass Interpolation Filter (LPIF) In this approach, a time invariant finite impulse response (FIR) digital low pass filter is used to interpolate the channel estimates in every time slot. This approach is similar to that in [42] where an FIR low-pass filter with unit sample response equal to a truncated raised-cosine pulse is used for interpolation. Here, however, we use the approach described in [43] to design an optimum FIR low-pass filter for interpolation that will minimize the error between the interpolated channel estimates and its true value. This approach will be briefly described below. For full mathematical treatment, however, the reader is referred to [43].

We are given a sequence $x(l)$, the values of which are possibly nonzero only at $l = kL_s$ where $k = 0, \pm 1, \pm 2, \cdots$. The sequence $x(l)$ is considered as being a sampled version of an unknown, but bandlimited sequence $u(l)$

$$x(l) = \begin{cases} u(l), & l = kL_s, k = 0, \pm 1, \pm 2, \cdots, \\ 0, & \text{otherwise.} \end{cases} \tag{49}$$

The sequence $u(l)$ is assumed to be bandlimited with

$$U(\omega) = 0 \quad \text{for} \quad |\omega| \geq \delta \cdot \pi / L_s, 0 < \delta \leq 1. \tag{50}$$

The sequence $x(l)$ here corresponds to the channel samples at the pilot positions. Let us assume that $g(l)$ is the unit sample response of the FIR interpolating filter, which, given every L_s sample of the sequence $u(l)$, interpolates the remaining $L_s - 1$ samples using K past and K future samples. It is easy to verify that the length of the filter will be then $2KL_s + 1$. The unit sample response $g(l)$ is designed such that the error

$$\varepsilon^2 = \sum_l ||(x * g)(l) - u(l)||^2 \tag{51}$$

is minimized. The method in [43] divides $g(l)$ into L_s subsequences $g_\mu(k) = g(kL_s + \mu), \mu = 0, 1, \cdots, L_s - 1, k = 0, \pm 1, \pm 2, \cdots$. The minimization of (51) results in the following set of linear equations for each μ

$$\sum_{m=-K}^{K-1} g_\mu(m)\phi((m-k)L_s) = \phi(kL_s + \mu) k = -K, \cdots, K-1 \quad \text{and } \mu = 0, 1, \cdots, L_s - 1 \tag{52}$$

where $\phi(n)$ is the autocorrelation function of $u(l)$ and is given by

$$\phi(n) = \int_{-\delta\pi/L_s}^{\delta\pi/L_s} |U(\omega)|^2 e^{-j\omega n}\, d\omega. \tag{53}$$

Equation (52) can be put in a matrix form as

$$\boldsymbol{\Phi} \boldsymbol{g}_\mu = \boldsymbol{\phi}_\mu \tag{54}$$

where

$$\boldsymbol{\Phi} = \begin{bmatrix} \phi(0) & \phi(L_s) & \cdots & \phi((2K-1)L_s) \\ \phi(L_s) & \phi(0) & \cdots & \phi((2K-2)L_s) \\ \vdots & \vdots & \ddots & \vdots \\ \phi((2K-1)L_s) & \phi((2K-2)L_s) & \cdots & \phi(0) \end{bmatrix}$$

is a Toeplitz matrix that does not depend on μ. Furthermore

$$\boldsymbol{g}_\mu = [g(-KL_s + \mu) g(-(K-1)L_s + \mu), \cdots, g((K-1)L_s + \mu)]^T$$
$$\boldsymbol{\phi}_\mu = [\phi(-KL_s + \mu) \phi(-(K-1)L_s + \mu), \cdots, \phi((K-1)L_s + \mu)]^T.$$

This, in some sense, resembles the WIF approach described above, except that the same filter is used for all points in the slot as compared to the WIF, in which a different filter (or set of weights) is used for each point in the slot. Also, since we require the filter to be time invariant, the filter bandwidth should satisfy the condition in (45) for the worst case maximum Doppler frequency and frequency offset. As explained above, this will degrade the performance at low f_d and f_d. In addition, since the receiver estimates the CSI in any given time slot using the pilot and training sequences in that slot only, interpolated CSI near the ends of the slot will exhibit a larger MSE than those near the middle of the slot.

IV. Simulation Results

In this section, we present the simulation results for the STCM-based modem architecture described above. These results will be presented for both the 8-PSK 32-state and the 16-QAM 16-state ST codes presented in Section II. We will briefly describe the simulation scenario in Sections IV-A and IV-B. The results of these simulations are presented in Sections IV-C through IV-G.

A. Time Slot Structure and Signaling Format

In all of the simulations, we assume IS-136 *basic* channelization and framing, except that the slot structure of the STCM-based modem will be different. For the purpose of comparison, we will briefly describe the channelization and framing structure in IS-136. On each 30-kHz channel, the IS-136 standard defines 25 frames of data per second ($N_f = 25$), each of which is then further subdivided into six time slots ($N_s = 6$). Each time slot is of 6.667-ms duration and carries 162 modulation symbols (the raw symbol rate R_s is 24 300 symbols/s). These symbols, in turn, include, 130 symbols for data or speech and 32 symbols for synchronization and control overhead. Under normal operating conditions, a single user is provided with exactly two time slots per frame, which guarantees the user a symbol rate of $2 \times 130 \times 25 = 6500$ symbols per second. The IS-136 uses $\pi/4$-DQPSK for modulation, which supports two bits per symbol. This means that the net (*uncoded*) bit rate over a 30-kHz channel is 39 kb/s.

Fig. 9 shows the slot structure for the STCM-based modem with two transmit antennas, using IS-136 basic channelization and framing. As with the IS-136 standard, we also assume

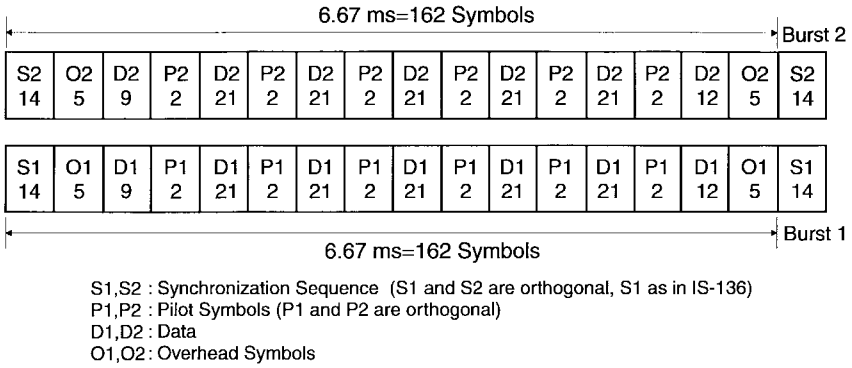

Fig. 9. Slot structure for STCM-based modem based on IS-136 timing and framing structure.

TABLE I
SNR$_w$(dB) USED FOR DESIGNING THE WIF'S FOR 8-PSK

1 Tx 1 Rx No ST code	2 Tx 1 Rx 32-State Code	2 Tx 2 Rx 32-State Code	2 Tx 1 Rx DD Code	2 Tx 2 Rx DD Code
25	20	12	30	17.5

TABLE II
SNR$_w$(dB) USED FOR DESIGNING THE WIF'S FOR 16-QAM

1 Tx 1 Rx No ST code	2 Tx 1 Rx 16-State Code	2 Tx 2 Rx 16-State Code
35	22.5	15

the same symbol rate R_s of 24 300 symbols/s. Each burst of 6.667 ms is 162 symbols long $(L_b = 162)$ and starts with a 14 symbols training sequence $(L_t = 14)$ that will be used for timing and frequency synchronization. The training sequence is also used to estimate the channel at the middle of the training sequence. In addition, the transmitter inserts six two-symbol $(N_p = 6, L_p = 2)$ pilot sequences $\boldsymbol{P}_1$ and $\boldsymbol{P}_2$ that are used for channel estimation. Thus, in each burst we are left with 136 symbols, ten of which will be reserved for control overhead and 126 of which will be used for information. The 126 symbols in each burst are interleaved by a 14×9 symbol-by-symbol block interleaver. The $\sqrt{\text{RC}}$ pulse shape $p(t)$ has a roll-off factor of 0.35.

B. Channel Estimation and Interpolation

As we pointed out before, signals at the receive antennas will be a linear superposition of the two transmitted bursts and we need the two training sequences $\boldsymbol{S}_1$ and $\boldsymbol{S}_2$, as well as the pilot sequences $\boldsymbol{P}_1$ and $\boldsymbol{P}_2$, to be orthogonal sequences. We use the same $\pi/4$-DQPSK synchronization sequence specified in the IS-136 standard for $\boldsymbol{S}_1$. This will allow the STCM-based service to coexist with old IS-136 services and, at the same time, ensure backward compatibility with IS-136.[4] We assume that the synchronization and pilot symbols have the same energy per symbol as the information symbols. As we mentioned before, in estimating the channel over any burst, the receiver uses the training and pilot sequences in that burst only since other time slots may be carrying bursts that correspond to old IS-136 wireless channels or other bursts with different structure. In addition, this will minimize the overall system delay. Thus, the receiver will use $\boldsymbol{S}_1$ and $\boldsymbol{S}_2$ at the beginning

[4]Some of today's IS-136 mobile phones use the synchronization sequence in other time slots to update their equalizer and maintain timing and frequency synchronization.

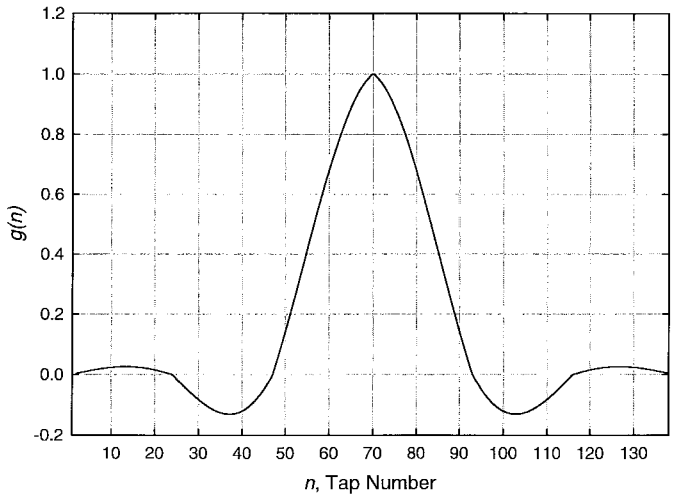

Fig. 10. Unit sample response of LPIF designed for $L_s = 23, K = 3$, and $\delta = 0.5$.

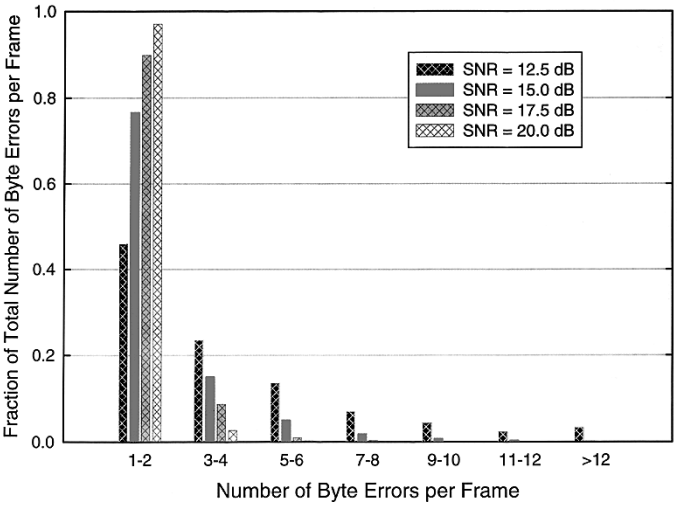

Fig. 11. Error histogram of the 16-QAM 16-state ST code without an outer RS with two transmit and two receive antennas and optimized WIF at $f_d = 180$ Hz.

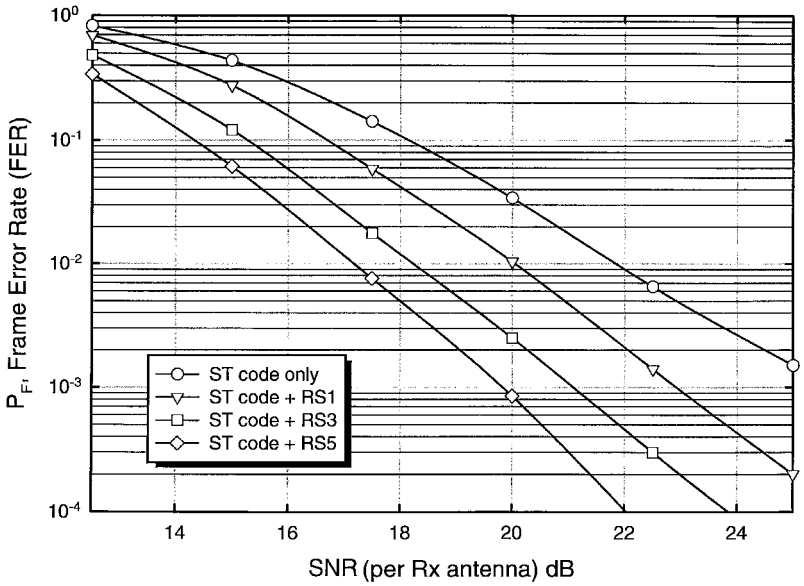

Fig. 12. Peformance of the 16-QAM 16-state ST code with two transmit and two receive antennas and $f_d = 180$ Hz.

of the current time slot, the six pilot sequences $\boldsymbol{P}_1$ and $\boldsymbol{P}_2$, as well as $\boldsymbol{S}_1$ and $\boldsymbol{S}_2$, at the beginning of the next time slot (which may belong to a different user) to obtain eight estimates per TDMA time slot $(N_e = 8)$ for the channel from each of the transmitting antennas to the receiver. The sampling period of these channel estimates $T_s' = L_s \cdot T_s$ where $L_s = 23$, in our case, can be easily seen to be 23/24 300 which corresponds to a sampling frequency $f_s' \approx 1056$Hz . In all of the simulations we will consider maximum Doppler frequencies up to 180 Hz, a residual frequency offset f_o of 200 Hz, an over sampling factor $Q = 8$, and a timing error δT_s which is uniformly distributed over $\pm T_s/16$. Thus, an f_s' of 1056 Hz will satisfy the requirement in (45).

For the WIF, we assumed that the 200-Hz Doppler range is divided into four subranges: 0–20, 20–80, 80–140, and 140–200 Hz. Four different WIF's were designed, one for each subrange. These filters were optimized at a frequency offset f_o of 200 Hz, maximum Doppler frequencies of 20, 80, 140, and 200 Hz, respectively, and an SNR_w that will depend on the ST code used and the number of transmit and receive antennas used. Tables I and II list the SNR_w used for designing the WIF's for both the 8-PSK and 16-QAM cases we considered.

For the LPIF, the approach described in Section III-G2 was used to design a time-invariant low-pass filter with $L_s = 23, K = 23, \delta = 0.5$. Fig. 10 shows the unit sample response $g(n)$ of the LPIF. The low-pass filter was designed such that it will have its 3-dB cutoff frequency at 528 Hz.

C. 16-QAM Results

For the 16-QAM 16-state space time code, shown in Fig. 3, we simulated the STCM-based modem without an outer RS code. Fig. 11 shows the number of errors per frame as a fraction of the total number of errors per frame for two transmit and two receive antennas at a maximum Doppler frequency $f_d = 180$ Hz. From this figure we can easily see that for SNR's of more than 15 dB, more than 80% of the frame errors are due to one or two symbol errors and 90% of them are due to four or fewer symbol errors. These errors can be corrected by using a high-rate outer code. Therefore, we considered three different shortened RS codes over $GF(2^8)$ for the outer code. The first

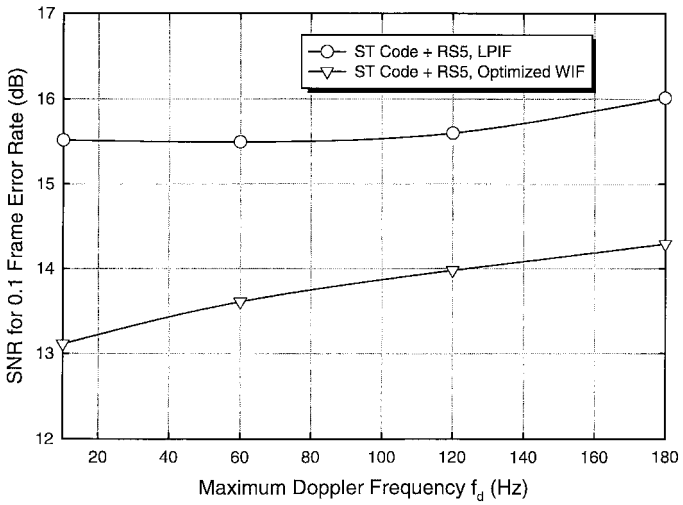

Fig. 13. SNR performance at 10% FER as a function of f_d of the 16-QAM 16-state ST code with two transmit and two receive antennas.

TABLE III
SNR (dB) REQUIRED FOR 10% FER FOR THE 16-QAM 16-STATE ST CODE FOR DIFFERENT BIT RATES

Maximum Doppler Frequency f_d	Diversity	ST Code (74.4 kbps)	ST Code + RS3 (67.2 kbps)	ST Code + RS5 (62.4 kbps)
10 Hz	2Tx 1Rx	22.4	21.1	20.5
	2Tx 2Rx	15.7	13.8	13.2
	1Tx 1Rx	**28.0**	**25.6**	**24.6**
	1Tx 2Rx	**20.7**	**18.1**	**17.5**
180 Hz	2Tx 1Rx	30.6	25.0	23.0
	2Tx 2Rx	18.1	15.3	14.3
	1Tx 1Rx	**> 50**	**32.4**	**28.9**
	1Tx 2Rx	**24.5**	**20.3**	**18.9**

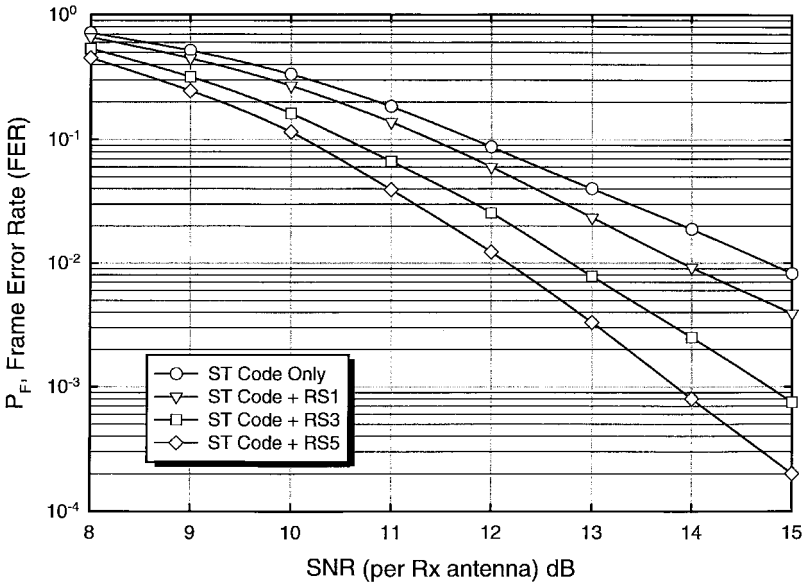

Fig. 14. Performance of the 8-PSK 32-state ST code with two transmit and two receive antennas and $f_d = 180$ Hz.

code, referred to as RS1, is a shortened RS(62, 60) code that corrects single-byte errors. The second RS code, referred to as RS3, is a shortened RS(62, 56) code that corrects three-byte errors, and the third RS code, referred to as RS5, is a shortened RS(62, 52) code that corrects five-byte errors. For RS1, for example, the $62GF(2^8)$ symbols are first created by partitioning a block of 480 information bits into 60 groups of eight bits each. These 60 bytes are then encoded by RS1 to give 62 bytes or RS symbols. The output $62GF(2^8)$ symbols $(62 \times 8 = 496$ bits) are then partitioned into 124 16-QAM symbols, two modulation symbols per one RS symbol. The 124 16-QAM symbols are then padded with two 16-QAM zero symbols to force the ST encoder to go back to the zero state.[5] The 126 16-QAM symbols are then encoded using the ST encoder.

Fig. 12 shows the FER performance of the 16-QAM 16-state ST code with two transmit and two receive antennas and a maximum Doppler frequency $f_d = 180$ using optimized WIF. From this figure we can see that the ST code alone needs an SNR of 18 dB to achieve 10% FER. However, when the ST code is concatenated with RS5, for example, the required SNR is 14.5 dB, which is a 3.5-dB gain over the ST code alone. In this case, however, the net bit rate (over a 30-kHz channel) at 10% FER will be reduced from 74.4 kb/s to 62.4 kb/s. Fig. 13 shows the SNR required for 10% FER versus the maximum Doppler frequency f_d for the 16-QAM 16-state ST code, concatenated with RS5 and two transmit and two receive antennas. We plot the results for both the LPIF and WIF. We can easily see a 2.5–3.5 dB advantage for the WIF over the LPIF for maximum Doppler frequencies up to 180 Hz. As expected, the WIF will have a better performance than the LPIF (since we are optimizing the filter coefficients for every point in the slot), although it would be more computationally expensive and would require more memory to store the coefficients.

[5]For the 16-QAM 16-state ST code only one 16-QAM zero symbol is needed to terminate the trellis, the other symbol is merely a dummy symbol.

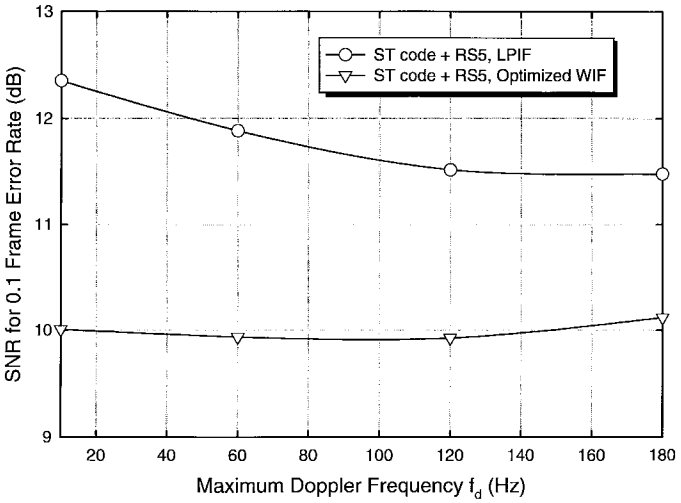

Fig. 15. SNR performance at 10% FER as a function of f_d of the 8-PSK 32-state ST code with two transmit and two receive antennas.

TABLE IV
SNR (dB) REQUIRED FOR 10% FER FOR THE EIGHT-PSK 32-STATE ST CODE FOR DIFFERENT BIT RATES

Maximum Doppler Frequency	Diversity	ST Code (55.8 kbps)	ST Code + RS3 (50.4 kbps)	ST Code + RS5 (46.8 kbps)
10 Hz	2Tx 1Rx	18.3	17.3	16.9
	2Tx 2Rx	11.2	10.3	10.1
	1Tx 1Rx	**25.5**	**23.1**	**22.0**
	1Tx 2Rx	**18.4**	**15.8**	**14.9**
180 Hz	2Tx 1Rx	20.1	17.6	17.1
	2Tx 2Rx	11.8	10.6	10.2
	1Tx 1Rx	**41.0**	**28.5**	**25.4**
	1Tx 2Rx	**21.9**	**17.6**	**16.2**

Table III summarizes the SNR performance at 10% FER for the 16-QAM 16-state ST code case. It shows the required

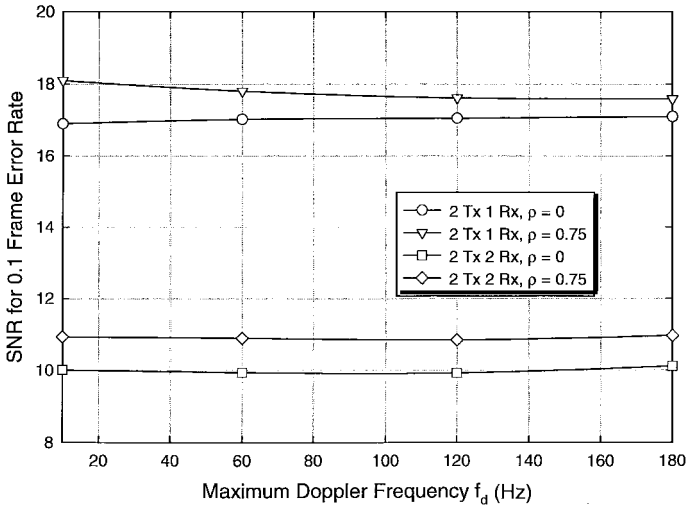

Fig. 16. Effect of transmit antenna correlation on the SNR performance at 10% FER for the 8-PSK 32-state ST code as a function of f_d.

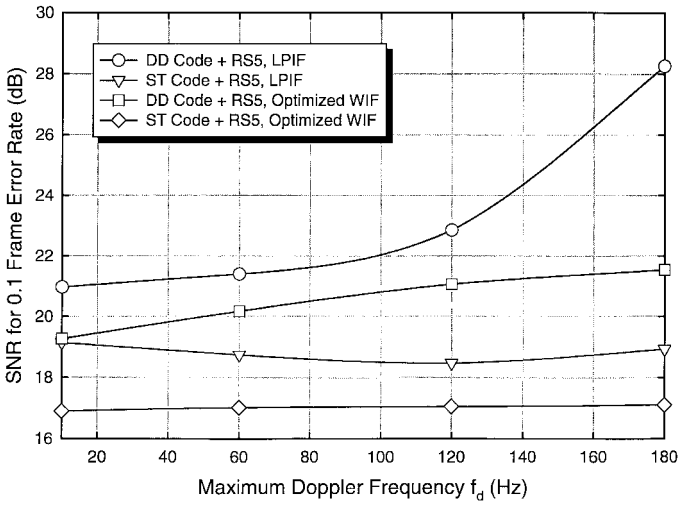

Fig. 17. SNR performance at 10% FER. Performance of delay diversity versus 8-PSK 32-state ST code with two transmit and one receive antennas as a function of f_d.

SNR for different number of transmit and receive antennas and different bit rates, for maximum Doppler frequencies of 10 and 180 Hz. For all of these cases we assumed that the WIF is used for to obtain the interpolated CSI. In addition, we also included the case when there is only one transmit antenna as a reference at the transmitter, which corresponds to the case where no ST coding is used. From these numbers, one can easily see the improvement in the SNR performance due to the use of the ST code with transmit antennas. For example, when using the space time code alone with two transmit and one receive antennas, at a maximum Doppler frequency of 10 Hz, an improvements of 5.6 dB (over the system with one transmit and one receive antenna) is achieved. For the same case, at a maximum Doppler frequency of 180 Hz, this improvement is even larger at more than 20 dB.

D. 8-PSK Results

For the 8-PSK constellation, we considered the same three RS codes used for the 16-QAM case, except that the code polynomial is now defined over $GF(2^6)$ and each symbol is 6 bits long. For RS1, in this case, the 62 $GF(2^6)$ symbols are first created by partitioning a block of 360 information bits into 60 groups of 6 bits each. The output 62 $GF(2^6)$ symbols are then partitioned into 124 8-PSK symbols, two modulation symbols per one RS symbol. The 124 8-PSK symbols are then padded with two 8-PSK zero symbols to force the ST encoder to go back to the zero state. The 126 8-PSK symbols are then encoded using the ST encoder.

Fig. 14 shows the FER performance of the 8-PSK 32-state ST code with two transmit and two receive antennas and $f_d = 180$ with WIF. From this figure, we can see that a 10% FER can be achieved at 11.7-dB SNR and 10-dB SNR with an 8-PSK 32-state ST code, concatenated with RS1 and RS5, respectively. This corresponds to a net bit rate (over a 30-kHz channel) of 54 kb/s and 46.8 kb/s, respectively. Fig. 15 shows the SNR required for 10% FER versus f_d for the 8-PSK 32-state ST code, concatenated with RS5 and two receive antennas. As in the 16-QAM 16-state ST code case,

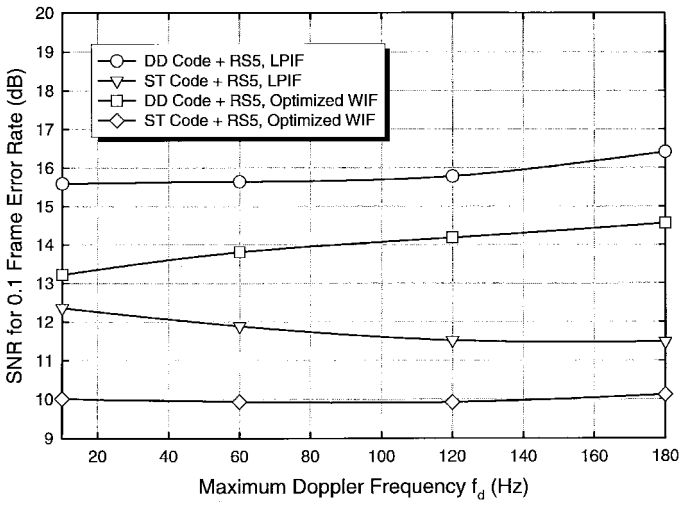

Fig. 18. SNR performance at 10% FER. Performance of delay diversity versus 8-PSK 32-state ST code with two transmit and two receive antennas as a function of f_d.

we also plot the results for both the LPIF and the WIF. We can see a 2.5-dB advantage for the WIF over the LPIF at 10 Hz. At 180 Hz, the WIF advantage over the LPIF is only 1.5 dB.

Table IV summarizes the SNR performance at 10% FER for the 8-PSK 32-state ST code case. It also shows the required SNR for different numbers of transmit and receive antennas and different bit rates, for maximum Doppler frequencies of 10 and 180 Hz. As before, we assume that the WIF is used to obtain the interpolated CSI. Similar to the 16-QAM case, we can easily see the improvement in the SNR, due to the use of the ST code, as compared to the case when only one transmit antenna is used (no ST coding).

E. Effect of Transmit Antenna Correlation

Next, we study the effect of transmit antenna correlation on the STCM-based modem performance. In this case, we

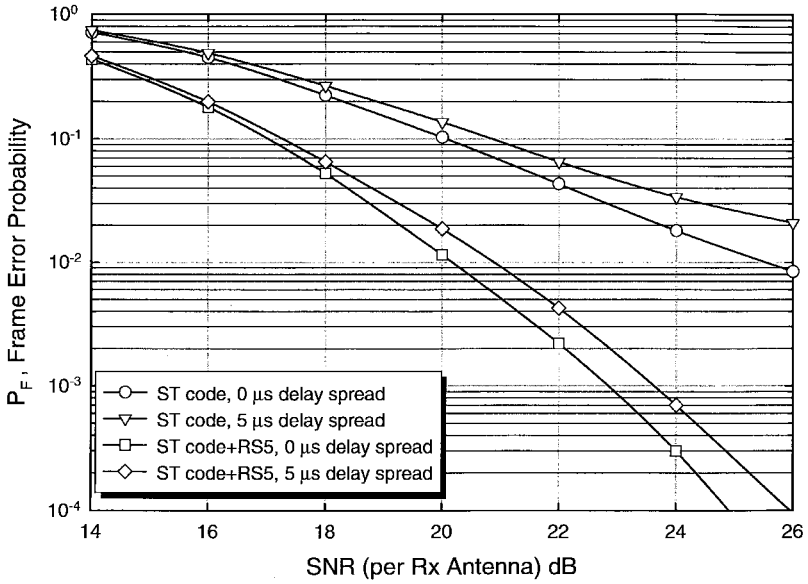

Fig. 19. Performance of the 8-PSK 32-state ST code with two transmit and one receive antennas at $f_d = 180$ Hz in a TU environment with delay spread of 5 μs (GSM TU channel model).

assumed that the channel gains from the two transmit antennas to the jth receive antenna are correlated such that

$$E\{\boldsymbol{\alpha}_j(l)\boldsymbol{\alpha}_j^*(l)\} = \begin{bmatrix} 1 & \rho \\ \rho & 1 \end{bmatrix}$$

where $\boldsymbol{\alpha}_j(l) = [\alpha_{1j}(l)\alpha_{2j}(l)]^T$. Fig. 16 also shows the SNR required for 10% FER as a function of the maximum Doppler frequency for $\rho = 0.75$ and $\rho = 0$ (*uncorrelated channel gains*) for the 8-PSK 32-state ST code with two transmit antennas. We can easily see that, even though the channels from the two transmit antennas are highly correlated, the performance was degraded by less than 1 dB for both the one- and two-receive antennas cases.

F. Performance of ST Coding Versus Delay Diversity

Here, we compare the performance of the STCM scheme versus the simple delay-diversity scheme. For that purpose, we consider the delay-diversity scheme with 8-PSK constellation. In this case the delay-diversity scheme will have the ST coding representation shown in Fig. 4. We simulated the STCM-based modem with the delay-diversity code shown in Fig. 4 as its ST code. Figs. 17 and 18 show the SNR required for 10% FER as a function of the maximum Doppler frequency f_d for the cases with one and two receive antennas, respectively. We show the results for both the WIF and the LPIF. We also show the corresponding results for the 8-PSK 32-state ST code. We can immediately see that the STCM scheme has an approximately 4-dB SNR advantage over simple delay diversity with two receive antennas for both the LPIF and the WIF. For one receive antenna and the WIF, the SNR advantage of STCM over simple delay diversity is about 2.5 and 4.5 dB for $f_d = 10$ and 180 Hz, respectively. For the one-receive antenna case and LPIF, this advantage goes up 9 dB at a maximum Doppler frequency of 180 Hz. The superior performance of the ST code over the delay-diversity scheme is due to the extra coding gain provided by the code.

TABLE V
THE GSM TU CHANNEL MODEL: DELAY SPREAD = 5 μs

Delay (μs)	0.0	0.2	0.5	1.6	2.3	5.0
Strength (dB)	-3.0	0.0	-2.0	-6.0	-8.0	-10.0

TABLE VI
THE GSM HT CHANNEL MODEL: DELAY SPREAD = 17 μs

Delay (μs)	0.0	0.1	0.3	0.5	15.0	17.0
Strength (dB)	0.0	-1.5	-4.5	-7.5	-6.0	-12.0

G. Performance in Delay Spread Channels

In all of our discussions and simulations so far we have assumed that $h_{ij}(t)$, the channel impulse response (CIR) from ith transmitting antenna to jth receiving antenna, is a frequency-flat channel. That is, the channel impulse response is assumed to be

$$h_{ij}(\tau;t) = \alpha_{ij}(t)\delta(\tau - \tau_o)$$

where $\alpha_{ij}(t)$ is the channel gain defined earlier and τ_o is the propagation delay. This model is generally valid as long as the delay spread of the channel is *much* less than the symbol period. Measurements for typical urban (TU) and hilly terrain (HT) propagation environments, however, show delay spreads of up to 5 and 17 μs [44], respectively. In this case, the CIR will be

$$h_{ij}(\tau;t) = \sum_{u=1}^{U} \alpha_{ij,u}(t)\delta(\tau - \tau_u)$$

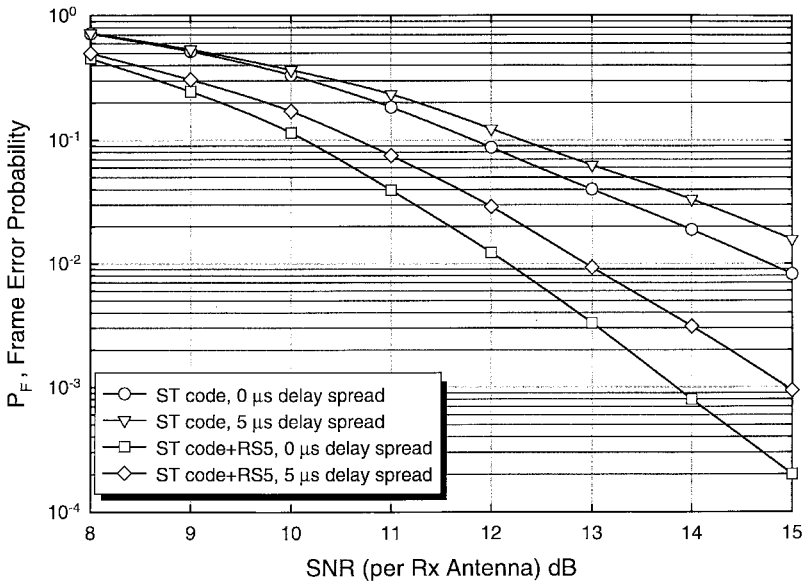

Fig. 20. Performance of the 8-PSK 32-state ST code with two transmit and two receive antennas at $f_d = 180$ Hz in a TU environment with delay spread of 5 μs (GSM TU channel model).

where $\alpha_{ij,u}(t)$ and τ_u are the complex channel gain and propagation delay for the uth multipath component.

Tables V and VI show the GSM measurement-based channel models for TU and HT channels [44]. We simulated the STCM-based modem described above with the 8-PSK 32-state space time code for both the TU and HT channel models. Figs. 19 and 20 show the FER performance for the STCM model with one and two receive antennas at a maximum Doppler frequency of 180 Hz and a TU channel model with 5 μs delay spread, respectively. From these two figures, we can easily see that for the TU channel model, and at $f_d = 180$ Hz, the performance degradation due to the multipath is 0.5 dB or less at an FER of 10%. Fig. 21 shows the SNR performance at 10% FER for the STCM-based modem using the TU channel model, which shows a performance degradation (at 10% FER) of less than 0.5 dB for the one receive antenna case and less than 1 dB for the two receive antenna case. For the HT channel model, however, the results showed a substantial error flooring due to the severe ISI caused by the channel. In this case it is very clear that an equalizer must be used, which is currently under investigation.

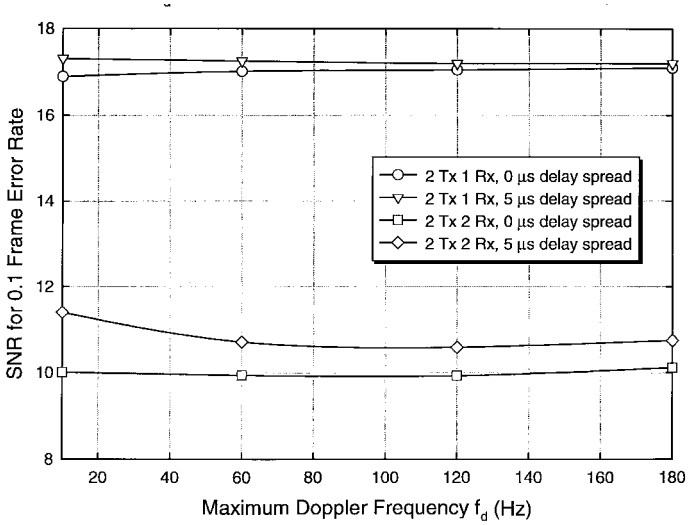

Fig. 21. Effect of delay spread on the SNR performance at 10% FER, or the 8-PSK 32-state ST code as a function of f_d.

V. Discussion and Conclusion

We have proposed a new advanced modem technology for high-data-rate wireless communications. This technology is based on the use of concatenated STCM with multiple transmit and/or multiple receive antennas. The spatial and temporal properties of STCM guarantee that, unlike with other transmit diversity techniques, diversity is achieved at the transmitter while maintaining optional receive diversity, without any sacrifice in transmission rate. The multichannel CSI required at the receiver for decoding is estimated using O-PSI techniques. A detailed design for a narrowband TDMA/STCM-based modem has been presented. Simulation results for the proposed STCM-based modem show great promise for STCM techniques as a powerful channel coding method for high-data-rate wireless applications. For example, the 16-QAM 16-state STCM-based modem with two transmit and two receive antennas, presented earlier, can achieve a net bit rate of 74.4 kb/s with 10% FER at SNR of 16 dB which is a 2.6 times increase in data rate, as compared to the net bit rate of 28.8 kb/s offered by the current IS-136 [45]. In addition, the STCM modem achieves these bit rates at an SNR that is lower than that required by current systems [45]. Simulation results also showed that the STCM-based modem performs well even when there is a correlation between the two transmit antennas, which suggests that the same concept can be easily applied at both base stations and handsets. In addition, the performance of the STCM-based modem in a typical urban propagation environment was very close to that under a frequency-flat channel response. For propagation environments

with large delay spreads ($\geq T_s/4$), however, multichannel equalization is necessary in order to maintain the performance of the STCM-based modem at acceptable levels. Efforts to design good multichannel equalizers for STCM are now under investigation. Research on the interaction and combination of STCM with other techniques, such as orthogonal frequency division multiplexing (OFDM), maximum likelihood (ML) decoding and interference cancellation, and beamforming is now being pursued [46]–[48].

ACKNOWLEDGMENT

The authors would like to thank the reviewers for their helpful comments and their thorough review. Their remarks greatly improved the presentation of the paper.

REFERENCES

[1] V. Tarokh, N. Seshadri, and A. R. Calderbank, "Space-time codes for high data rate wireless communications: Performance criterion and code construction," *IEEE Trans. Inform. Theory*, vol. 44, pp. 744–765, Mar. 1998.

[2] ——, "Space-time codes for high data rate wireless communications: Performance criterion and code construction," in *Proc. IEEE ICC'97*, Montreal, Canada, 1997, pp. 299–303.

[3] N. Seshadri, V. Tarokh, and A. R. Calderbank, "Space-time codes for high data rate wireless communications: Code construction," in *Proc. IEEE VTC'97*, Phoenix, AZ, 1997, pp. 637–641.

[4] V. Tarokh, A. F. Naguib, N. Seshadri, and A. R. Calderbank, "Space-time codes for high data rate wireless communications: Mismatch analysis," in *Proc. IEEE ICC'97*, Montreal, Canada, 1997, pp. 309–313.

[5] V. Tarokh, A. F. Naguib, N. Seshadri, and A. Calderbank, "Space-time codes for high data rate wireless communications: Performance criteria in the presence of channel estimation errors, mobility, and multiple paths," *IEEE Trans. Commun.*, to be published.

[6] N. Sollenberger and S. Kasturia, "Evolution of TDMA (Is-54/IS-136) to foster further growth of PCS," in *Proc. ICUPC Int. Conf. Universal Personal Communications, 1996*, Boston, MA, 1996.

[7] "Special issue on the European path toward UMTS," *IEEE Personal Commun. Mag.*, vol. 2, Feb. 1995.

[8] J. G. Proakis, "Adaptive equalization for TDMA digital mobile radio," *IEEE Trans. Veh. Technol.*, vol. 40, pp. 333–341, May 1991.

[9] R. Price and J. P. E. Green, "A communication technique for multipath channels," *Proc. IRE*, vol. 46, pp. 555–570, Mar. 1958.

[10] G. Turin, "Introduction to spread-spectrum antimultipath techniques and their application to urban digital radio," *Proc. IEEE*, vol. 68, pp. 328–353, Mar. 1980.

[11] P. S. Henry and B. S. Glance, "A new approach to high capacity digital mobile radio," *Bell Syst. Tech. J.*, vol. 51, no. 8, pp. 1611–1630, Sept. 1972.

[12] J. H. Winters, "Switched diversity with feedback for DPSK mobile radio systems," *IEEE Trans. Veh. Technol.*, vol. 32, pp. 134–150, Feb. 1983.

[13] G. J. Foschini and M. J. Gans, submitted for publication.

[14] G. Foscini, "Layered space-time architecture for wireless communication in a fading environment when using multi-element antennas," *AT&T Tech. J.*, vol. 1, Autumn 1996.

[15] A. Narula, M. Trott, and G. Wornell, submitted for publication.

[16] E. Teletar, "Capacity of multi-antenna Gaussian channels," AT&T Bell Laboratories, Murray Hill, NJ, Tech. Memo., 1995.

[17] A. Wittneben, "Base station modulation diversity for digital SIMULCAST," in *Proc. IEEE VTC'91*, St. Louis, MO, 1991, vol. 1, pp. 848–853.

[18] N. Seshadri and J. H. Winters, "Two schemes for improving the performance of frequency-division duplex (FDD) transmission systems using transmitter antenna diversity," *Int. J. Wireless Inform. Networks*, vol. 1, no. 1, pp. 49–60, Jan. 1994.

[19] A. Wittneben, "A new bandwidth efficient transmit antenna modulation diversity scheme for linear digital modulation," in *Proc. IEEE ICC'93*, Geneva, Switzerland, vol. 3, pp. 1630–1634.

[20] J.-C. Guey, M. P. Fitz, M. R. Bell, and W.-Y. Kuo, "Signal design for transmitter diversity wireless communication systems over Rayleigh fading channels," in *Proc. IEEE VTC'96*, Atlanta, GA, vol. 1, pp. 136–140.

[21] J. H. Winters, "Diversity gain of transmit diversity in wireless systems with Rayleigh fading," in *Proc. IEEE ICC'94*, New Orleans, LA, vol. 2, pp. 1121–1125.

[22] ——, "Diversity gain of transmit diversity in wireless systems with Rayleigh fading," *IEEE Trans. Veh. Technol.*, vol. 47, pp. 119–123, Feb. 1998.

[23] A. Hiroike, F. Adachi, and N. Nakajima, "Combined effects of phase sweeping transmitter diversity and channel coding," *IEEE Trans. Veh. Technol.*, vol. 41, pp. 170–176, May 92.

[24] T. Hattori and K. Hirade, "Multitransmitter simulcast digital signal transmission by using frequency offset strategy in land mobile radiotelephone," *IEEE. Trans. Veh. Technol.*, vol. VT-27, pp. 231–238, 1978.

[25] V. Weerackody, "Diversity for the direct-sequence spread spectrum system using multiple transmit antennas," in *Proc. ICC'93*, Geneva, Switzerland, May, 1993, vol. 3, pp. 1503–1506.

[26] J. K. Cavers, "An analysis of pilot symbol assisted modulation for Rayleigh faded channels," *IEEE Trans. Veh. Technol.*, vol. 40, pp. 683–693, Nov. 1991.

[27] S. Sampei and T. Sunaga, "Rayleigh fading compensation method for 16 QAM in digital land mobile radio channels," in *Proc. IEEE VTC'89*, San Francisco, CA, May 1989, vol. I, pp. 640–646.

[28] M. L. Moher and J. H. Lodge, "TCMP-A modulation and coding strategy for Rician fading channels," *IEEE J. Select. Areas Commun.*, vol. 7, pp. 1347–1355, Dec. 1989.

[29] R. J. Young, J. H. Lodge, and L. C. Pacola, "An implementation of a reference symbol approach to generic modulation in fading channels," in *Proc. Int. Mobile Satellite Conf.*, Ottawa, Canada, June 1990, pp. 182–187.

[30] J. Yang and K. Feher, "A digital Rayleigh fade compensation technology for coherent OQPSK System," in *Proc. IEEE VTC'90*, Orlando, FL, May 1990, pp. 732–737.

[31] C. L. Liu and K. Feher, "A new generation of Rayleigh fade compensated $\pi/4$-QPSK coherent modem," in *Proc. IEEE VTC'90*, Orlando, FL, May 1990, pp. 482–486.

[32] A. Aghamohammadi, H. Meyr, and G. Asheid, "A new method for phase synchronization and automatic gain control of linearly modulated signals on frequency-flat fading channel," *IEEE Trans. Commun.*, vol. 39, pp. 25–29, Jan. 1991.

[33] W. C. Jakes, *Microwave Mobile Communications*. New York: Wiley, 1974.

[34] J. G. Proakis, *Digital Communications*, 2nd ed. New York: McGraw-Hill, 1989.

[35] R. A. Horn and C. R. Johnson, *Matrix Analysis*. Cambridge: Cambridge Univ. Press, 1985.

[36] E. Biglieri, D. Divsalar, P. J. McLane, and M. K. Simon, *Introduction to Trellis Coded Modulation with Applications*. New York: Maxwell Macmillan, 1991.

[37] F. D. Natali, "AFC tracking algorithms," *IEEE Trans. Commun.*, vol. COM-32, pp. 935–947, Aug. 1984.

[38] S. Sampei and T. Sunaga, "Rayleigh fading compensation method for QAM in digital land mobile radio channels," *IEEE Trans. Veh. Technol.*, vol. 42, pp. 137–147, May 1993.

[39] J. Cioffi, "Digital communication," class notes, Stanford University, 1996.

[40] K. Feher, *Digital Communications Sattelite/Earth Station Engineering*. Englewood Cliffs, NJ: Prentice-Hall, 1981.

[41] G. H. Golub and C. F. V. Loan, *Matrix Computations*, 2nd ed. Baltimore, MD: Johns Hopkins Press, 1989.

[42] N. W. K. Lo, D. D. Falconer, and A. U. H. Sheikh, "Adaptive equalization and diversity combining for mobile radio using interpolated channel estimates," *IEEE Trans. Veh. Technol.*, vol. 40, pp. 636–645, Aug. 1991.

[43] G. Oetken and T. W. Parks, "New results in the design of digital interpolators," *IEEE Trans. Acoustics, Speech, Signal Processing*, June 1975, pp. 301–309.

[44] K. Pahlavan and A. H. Levesque, *Wireless Information Networks*. New York: Wiley, 1995.

[45] E. Gelblum and N. Seshadri, "High-rate coded modulation schemes for 16 Kbps speech in wireless systems," in *Proc. 1997 47th IEEE Vehicular Technology Conf.*, Phoenix, AZ, May 1997, pp. 349–353.

[46] V. Tarokh, A. F. Naguib, N. Seshadri, and A. R. Calderbank, "Array signal processing and space–time coding for very high data rate wireless communications," submitted for publication.

[47] A. F. Naguib, N. Seshadri, V. Tarokh, and S. Alamouti, "Combined interference cancellation and ML decoding of block space–time codes," submitted for publication.

[48] D. Agrawal, V. Tarokh, A. F. Naguib, and N. Seshadri, "Space-time coded OFDM for high data rate wireless communications over wideband channels," in *Proc. IEEE VTC'98*, Ottawa, Canada, May 1998.

Ayman F. Naguib (S'91–M'96) received the B.Sc. degree (with honors) and the M.S. degree in electrical engineering from Cairo University, Cairo, Egypt, in 1987 and 1990, respectively, and the M.S. degree in statistics and the Ph.D. degree in electrical engineering from Stanford University, Stanford, CA, in 1993 and 1996, respectively.

From 1987 to 1989, he served at the Signal Processing Laboratory, The Military Technical College, Cairo, Egypt. From 1989 to 1990, he was employed with Cairo University as a Research and Teaching Assistant in the Communication Theory Group, Department of Electrical Engineering. From 1990 to 1995, he was a Research and Teaching Assistant in the Information Systems Laboratory, Stanford University. In 1996, he joined AT&T Labs-Research, Florham Park, NJ, as a Senior Member of the Technical Staff. His current research interests include signal processing and coding for high-data-rate wireless and digital communications and modem design for broadband systems.

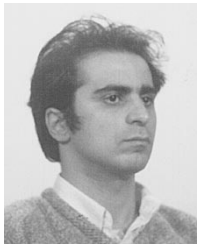

Vahid Tarokh (M'97) received the Ph.D. degree in electrical engineering from the University of Waterloo, Waterloo, Ontario, Canada, in 1995.

He is currently a Senior Member of the Technical Staff at AT&T Labs-Research, Florham Park, NJ.

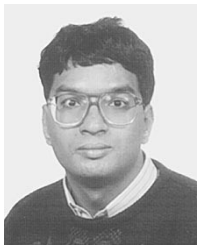

Nambirajan Seshadri (S'81–M'82–SM'95) received the B.S. degree in electronics and communications engineering from the University of Madras, Madaras, India, in 1982 and the M.S. and Ph.D. degrees in electrical and computer engineering from Rensselaer Polytechnic Institute, Troy, NY, in 1984 and 1986, respectively.

He was a Distinguished Member of the Technical Staff at AT&T Bell Laboratories, Murray Hill, NJ, and is now Head of the Communications Research Department at AT&T Labs-Research, Florham Park, NJ. His technical interests include coding and modulation, diversity techniques, and reliable transmission of audio-visual signals over wireless channels.

Dr. Seshadri has just completed his term as Associate Editor for Coding Techniques for the IEEE TRANSACTIONS ON INFORMATION THEORY.

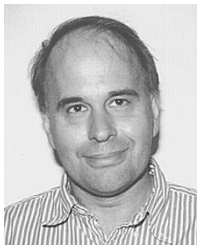

A. Robert Calderbank (M'89–SM'97–F'98) received the B.S. degree in mathematics from Warwick University, Coventry, U.K., in 1975, the M.S. degree in mathematics from Oxford University, Oxford, U.K., in 1976, and the Ph.D. degree in mathematics from the California Institute of Technology, Pasadena, in 1980.

He joined AT&T Bell Laboratories in 1980, and was a Department Head in the Mathematical Sciences Research Center at Murray Hill. He is currently Director of the Information Sciences Research Center at AT&T Labs-Research, Florham Park, NJ. His research interests include algebraic coding theory, wireless data transmission, and quantum computing. At the University of Michigan, and at Princeton University he developed and taught an innovative course on bandwidth-efficient communication.

Dr. Calderbank was the Associate Editor for Coding Techniques for the IEEE TRANSACTIONS ON INFORMATION THEORY from 1986 to 1989. He was also a Guest Editor for a Special Issue of the IEEE TRANSACTIONS ON INFORMATION THEORY dedicated to coding for storage devices. He served on the Board of Governors of the IEEE Information Theory Society from 1990 to 1996. He was a corecipient of the 1995 Prize Paper Award from the Information Theory Society for his work on the Z4 linearity of the Kerdock and Preparata codes. He is currently Editor-in-Chief of the IEEE TRANSACTIONS ON INFORMATION THEORY.